HELMHOLTZ RESEARCH FOR GRAND CHALLENGES

JÜLICH Forschungszentrum

Spectroscopy in Magnetic Confined Fusion Plasmas

PART I

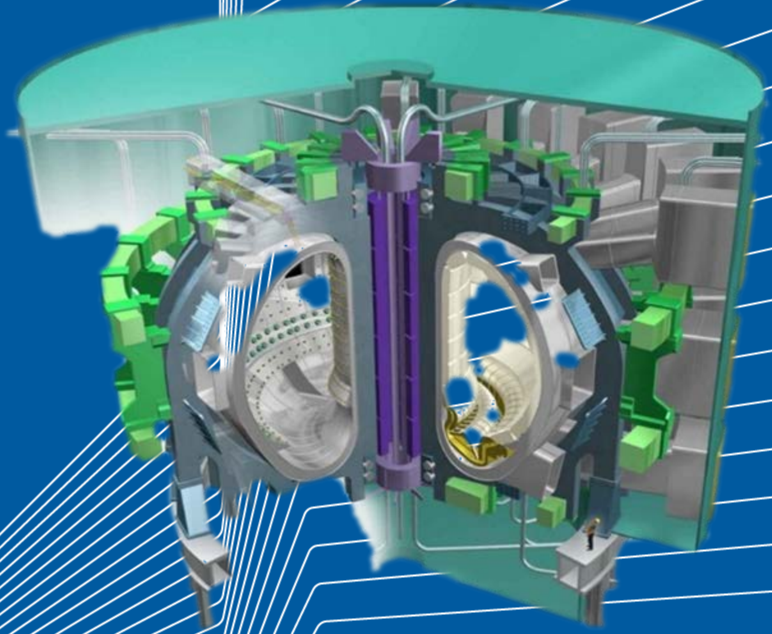

Sebastijan Brezinsek

Institut für Energie und Klimaforschung - Plasmaphysik
Forschungszentrum Jülich

Sun: a Cosmic Power Plant

Energy production in the sun by nuclear fusion of lightest elements: proton-proton (pp) cycle

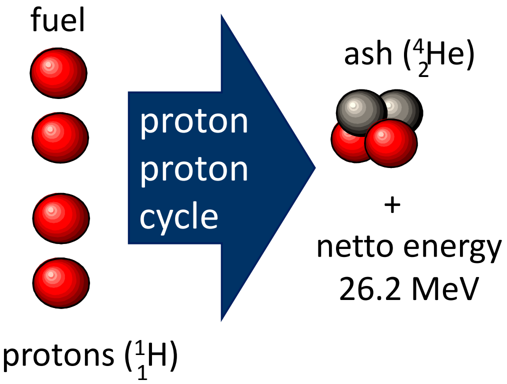

Mass defect in this reaction: 4.8×10^{-29} kg =>
1 kg of H produces 6.4×10^{14} J of energy

plasma
pressure: 1×10^{16} Pa = 1×10^{11} bar (core)
temperature: 1.3 keV (core)
density: 1×10^{32} m^{-3} (core)

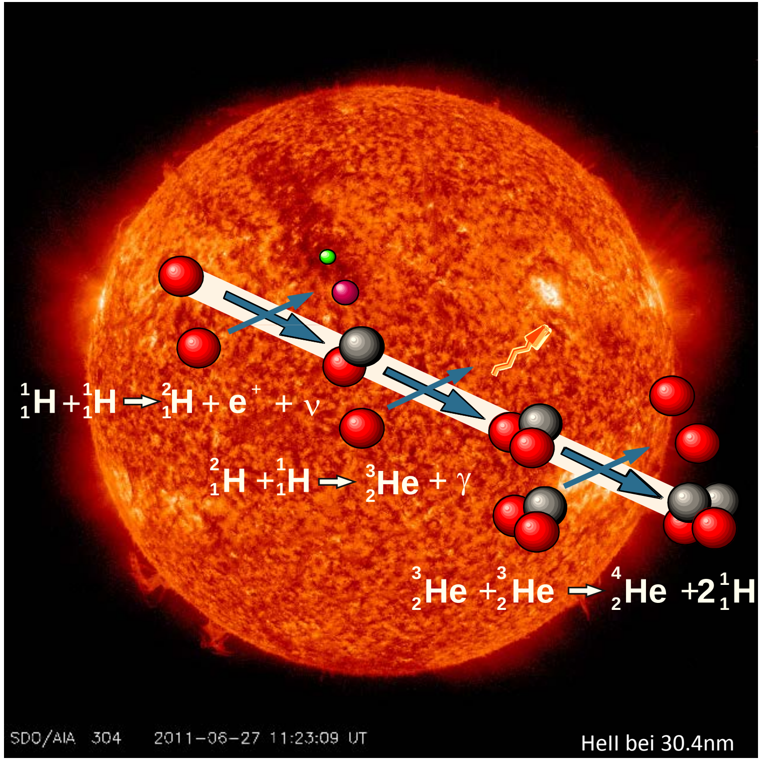

Inertial confinement (gravity)

Outline

- Introduction
- Tokamak functionality
  - Examples from spectroscopy in MCF
  - JET tokamak
  - W as plasma-facing material
- ITER
  - Set-up the larget machine in the world
  - ITER optical diagnostics
- W7-X
  - A further step in complexity

Nuclear Fusion Reactions and Reaction Partners

JÜLICH Forschungszentrum

- Nuclear fusion based on pp cycle not suitable on earth “to produce energy“
- Thermonuclear fusion with largest reaction rate: dt fusion reaction
- Inertial (ICF) and magnetically confined fusion (MCF) plasma studies are aiming in the exploitation of the DT reaction (on earth)

neutral particles	plasma	charged particles
		e electrons (-)
Neutron ($^{0}_{1}n$) **n**		
Hydrogen ($^{1}_{1}H$ =H)		**p** protons (+)
Deuterium ($^{2}_{1}H$ =D)		**d** deuterons (+)
Tritium ($^{3}_{1}H$ =T)		**t** tritons (+)
Helium ($^{4}_{2}He$)		α-particles (2+)

Spectroscopy of fuel H_2, D_2, T_2, HD, HT, DT molecules and H, D, T atoms and of fusion ash, He atoms and ions, required!

Maxwell-averaged reaction activity vs ion temperatures for fusion reactions

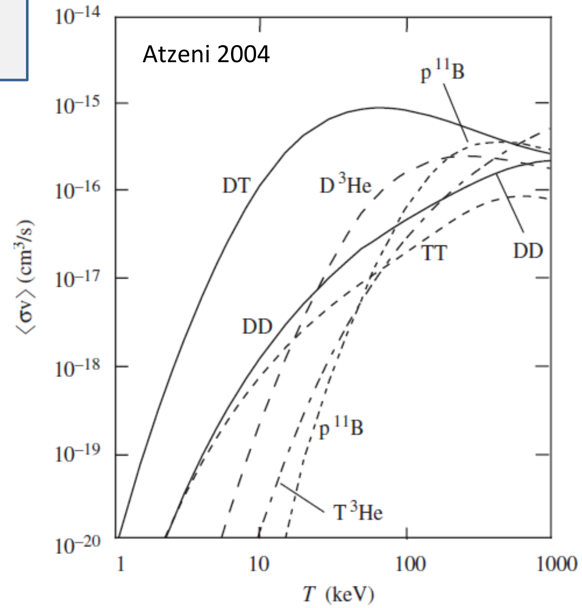

p-p reaction at 10^{-40} cm^{3}s^{-1} !

Example of Emission Spectra in Fusion Plasmas

D_2 and T_2 emission spectra (plasma edge)

Fulcher-α band

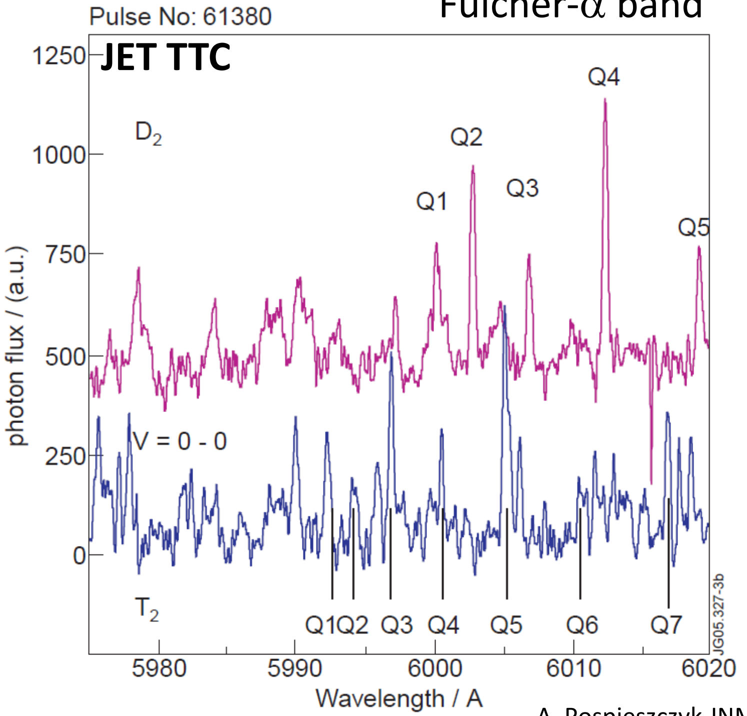

A. Pospieszczyk JNM 2007

H, D, T emission spectra (exhaust)

Balmer–α line

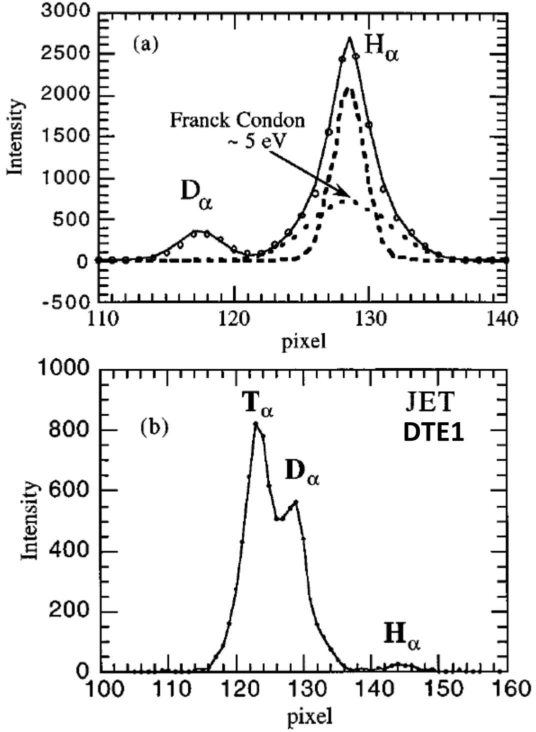

D. Hillis RSI 1999

Nuclear Fusion Reactions: DT

JÜLICH Forschungszentrum

Measure for the fusion power in a 50:50 DT reaction is the so-called triple product:

ion density (n_i) x ion temperature (T_i) x confinement time (τ_E)

Ignition in magnetically confined fusion plasmas achievable if:

$n_i\,[10^{20}\,m^{-3}]$ x $T_i\,[10keV]$ x $t_E\,[5s]$ $\geq$ $5x10^{21}$ keV s m^{-3} (Lawson criterion)

d + t → α + n + 17.6 MeV

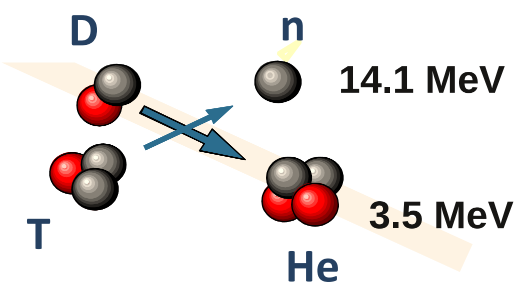

Requires D and T above 10keV, but the fuel starts as D_2 or T_2 gas or as DT ice pellet entering cold plasma in eV range.

- Spectroscopy from eV to keV range in one device
- Emission in the IR-VIS towards VUV-X-ray range

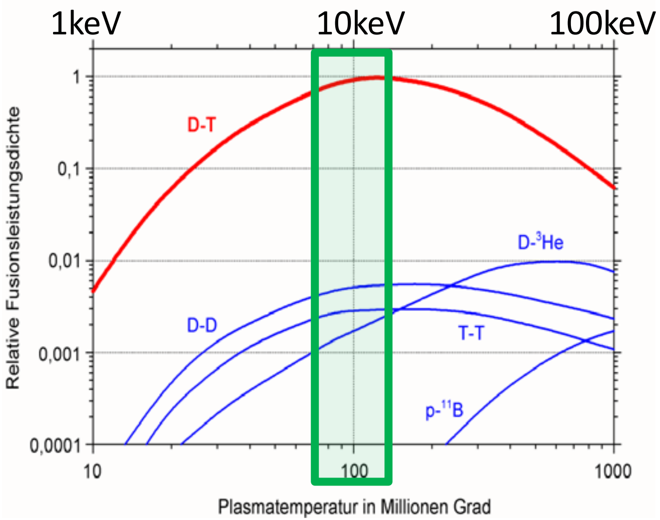

Nuclear Fusion Reactions: DT Fuel and Restrictions

Plasma densities in the range of 10^{27} m^{-3}-10^{32}m^{-3}

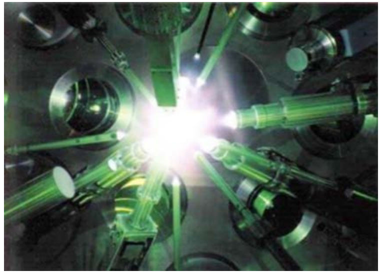

LASER-fusion (ICF)

inertia

plasma pressure $\nabla p = \rho \vec{g} + \vec{j} \times \vec{B}$

magnetic

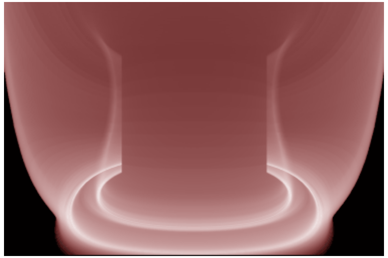

Magnetic confinement (MCF)

Plasma densities in the range of 10^{17}-10^{21} m^{-3}

D natural isotope in sea water: 0.015%

T must be breeded in a fusion reactor:

^{7}Li+n -> T + α + n‘ - 2.47 MeV

^{6}Li+n-> T+ α + 4.78 MeV

T is radioactive with a half-life of 12 years

Challenging environment (access)

- radioactive fuel
- first wall material activation
- neutron impact

Reduced number of spectroscopic techniques applicable

Particles in Magnetised Plasmas

Lorentz force acts on charged particles in a magnetic field:

$$\vec{F}_L = q \cdot \left[\vec{v} \times \vec{B}\right]$$ Lorentz force

Ions and electrons gyrate around magnetic field lines:

$$\left|\vec{r}_L\right| = \frac{\left|\vec{v}_\perp\right|}{\left|\vec{\omega}_L\right|} = \frac{mv_\perp}{qB}$$ Larmor radius

Many gyrations before a collisions occurs in magnetized plasmas:

$$\beta = \frac{\omega_L}{\upsilon_{collision}} >> 1$$ Hall parameter

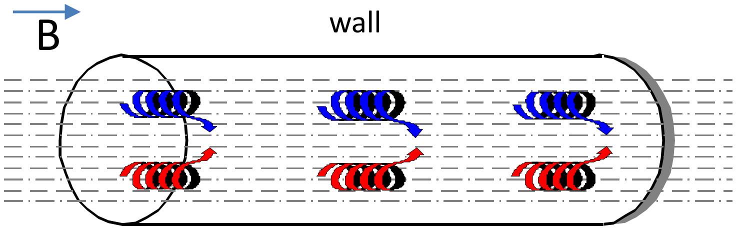

High mobility along magnetic field lines

Low mobility perpendicular magnetic field lines

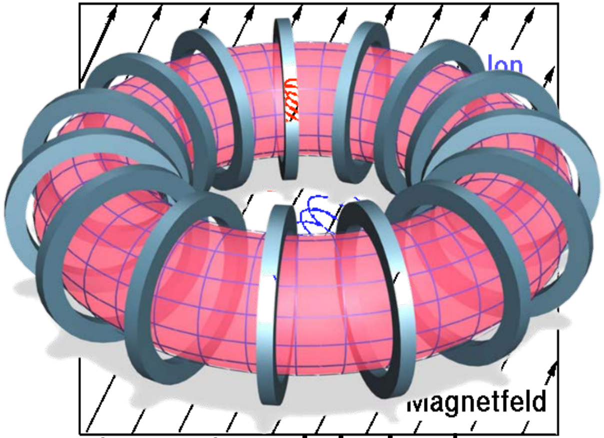

=> torus to minimise losses

Low plasma-wall interactions (PWI) if high magnetization present, full ionisation, and no-cross field transport (ideal case).

Spectroscopy at high magnetic fields with B>1T (line splitting)

Splitting and Observation of Spectral Lines

- Line splitting due to magnetic field strength (measure the local field): Zeeman and Paschen-Back effect
- Orientation of the observation with respect to the magnetic field important: σ and π components

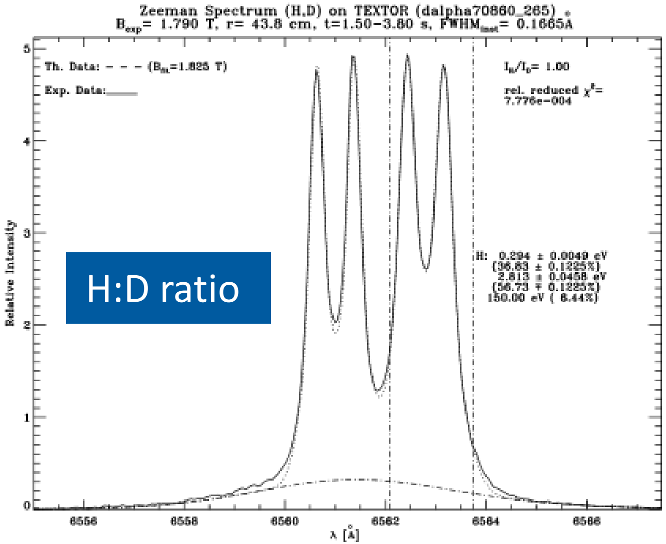

Hey CPP 2000

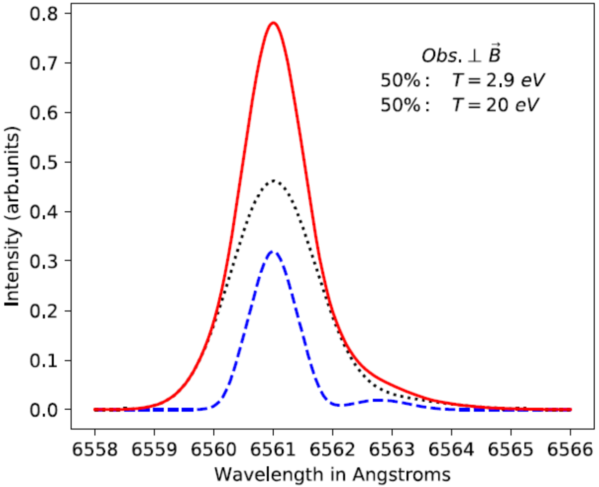

B=2T
95% D + 5% H

Koubiti Atom 2019

- Variables: energy of H atoms (origin of atoms), composition, and resolution of spectrometer
- Simulation tools available: x-paschen of ADAS suite etc.

Is a simple toroidal arrangement enough for MCF?

Particle drifts due to forces in (inhomogeneous) B-field:

$$\vec{v}_D = \frac{\vec{F} \times \vec{B}}{qB^2}$$

In torus geometry two inherent drifts appear:
∇B drift and curvature drift [so-called ”torus drift”]

$$\vec{v}_D = \frac{m}{qB^3}\left(v_\parallel^2 + \frac{1}{2}v_\perp^2\right)\vec{B} \times \nabla B$$

$$B_\phi = \frac{B_0 R_0}{R}$$

$$\vec{v}_D = \frac{\vec{E} \times \vec{B}}{B^2}$$

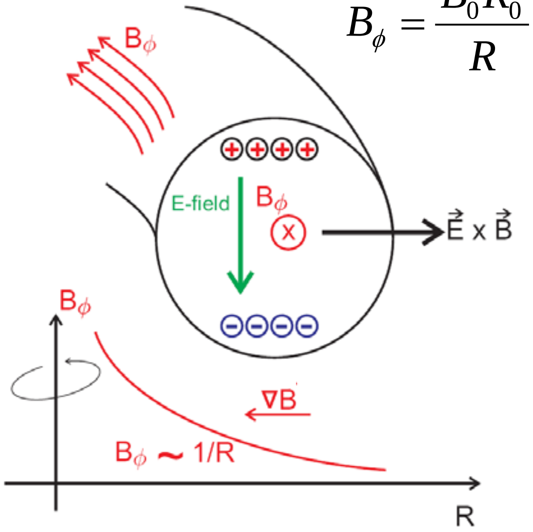

- Pure toroidal magnetic field induces charge separation due to “torus drift”
- Charge separation induces vertical electrical field E
- Electrical field E and magnetic field B induces E x B drift and movement of all particles outward to the wall
- Second magnetic field component required (poloidal direction) => induces screw-like trajectory (helical field lines) and stability

Spectroscopy at varying magnetic field strength:
High field side and low field side can be separated

Source Localisation by Spectrosopcy

- "Cold" atoms near wall surfaces: localization possible via spectroscopy
- Depends on magnetic field, plasma condition, energy composition, optical arrangement, geometry …

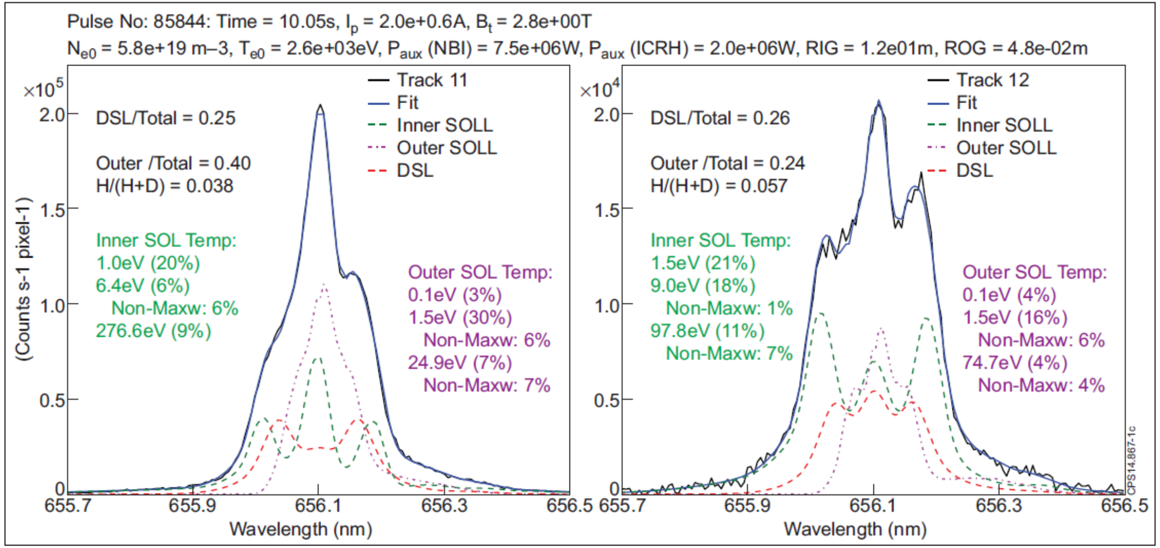

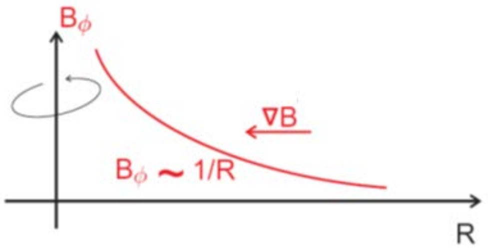

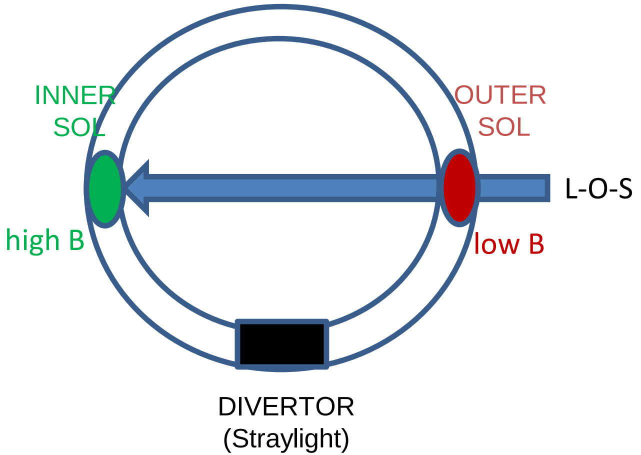

Metallic surface cause reflection – simulations required

Kukushkin IAEA2016

Magnetically Confined Fusion: Main Lines

Two ways to provide poloidal field component and helical field line structure

plasma current induces poloidal field

pure magnetic coil arrangement (solution)

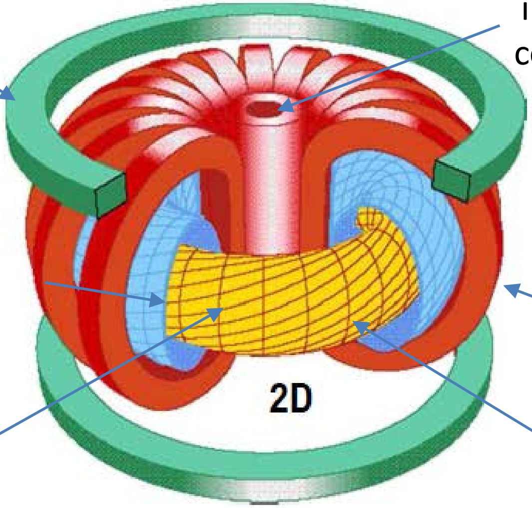

tokamak

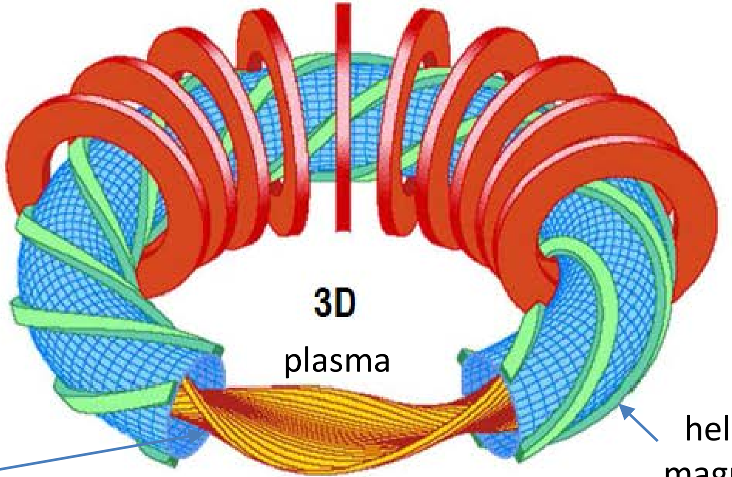

stellarator

in general: pulsed operation of device

in general: steady-state operation of device

Magnetically Confined Fusion: Tokamak Principle

Poloidal field component induced by plasma current resulting in helical, twisted magnetic field structure

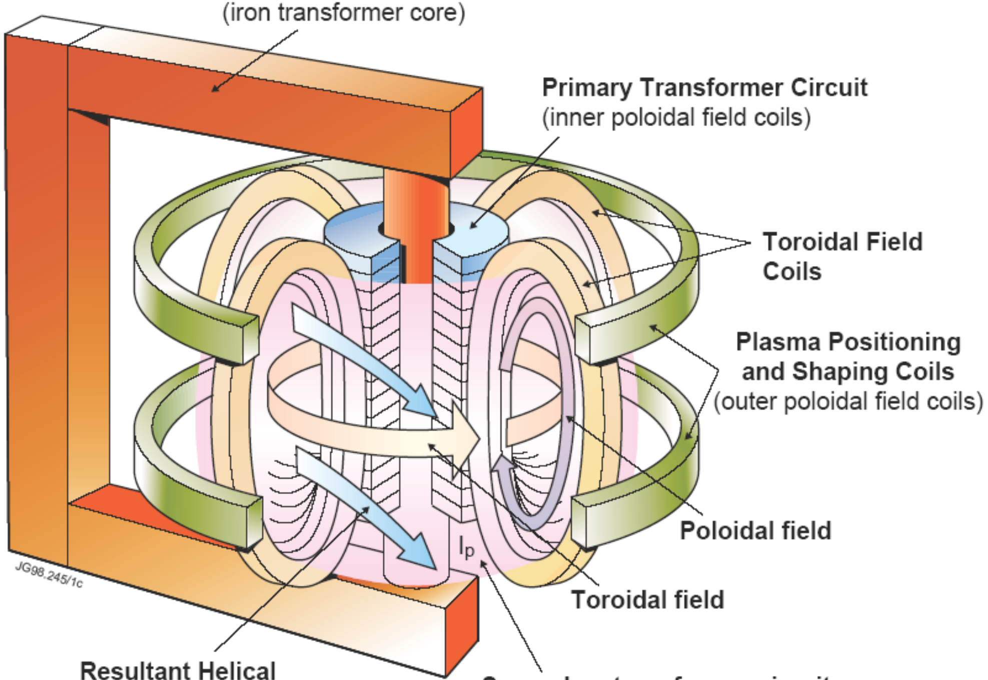

Induced poloidal magnetic field is about 1/10 of toroidal field

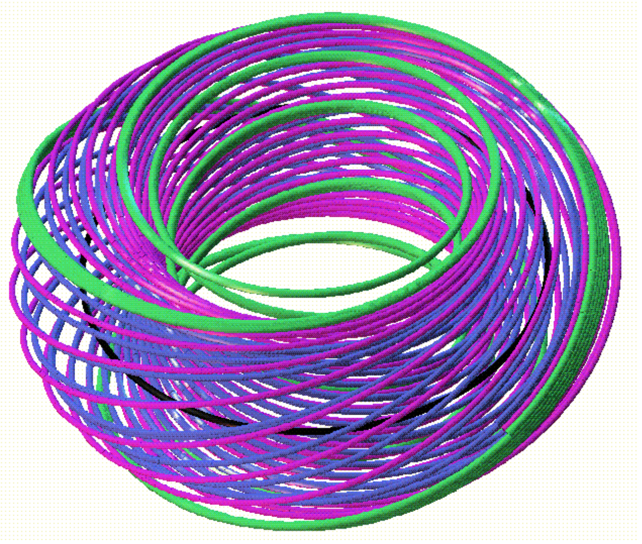

Joint European Torus: JET Tokamak

poloidal and 24 toroidal field coils

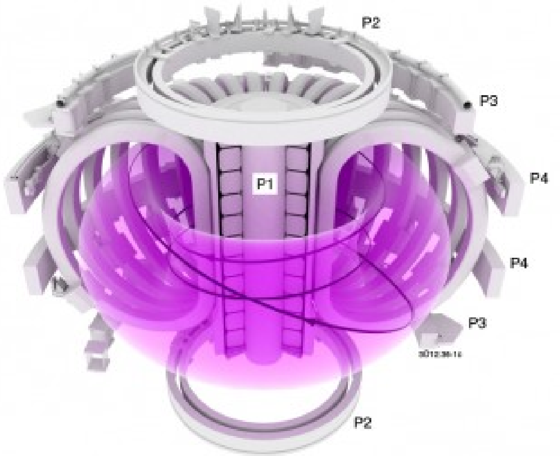

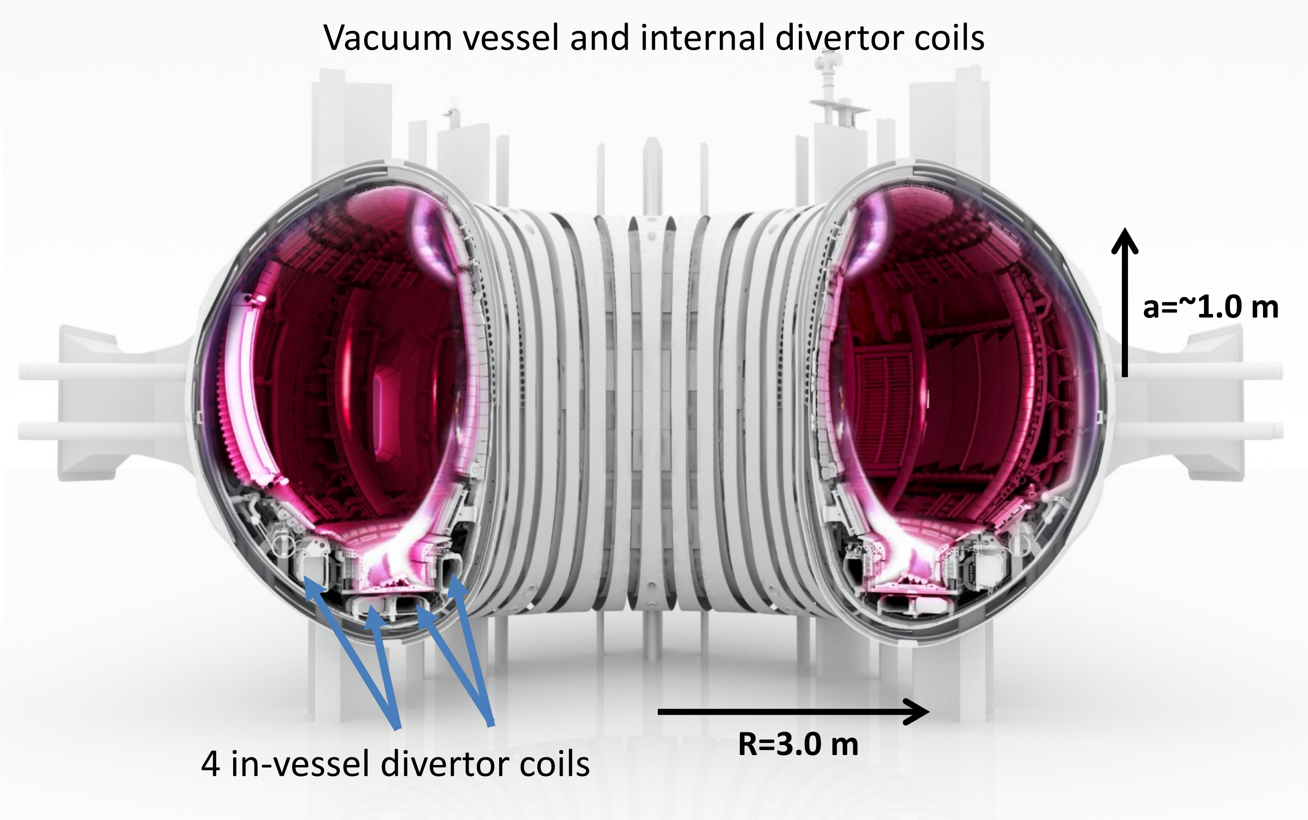

Joint European Torus: Discharge Example

Largest tokamak currently operating: up to 4.8MA plasma current, 3.45T at max. toroidal field, P_{aux}~40MW

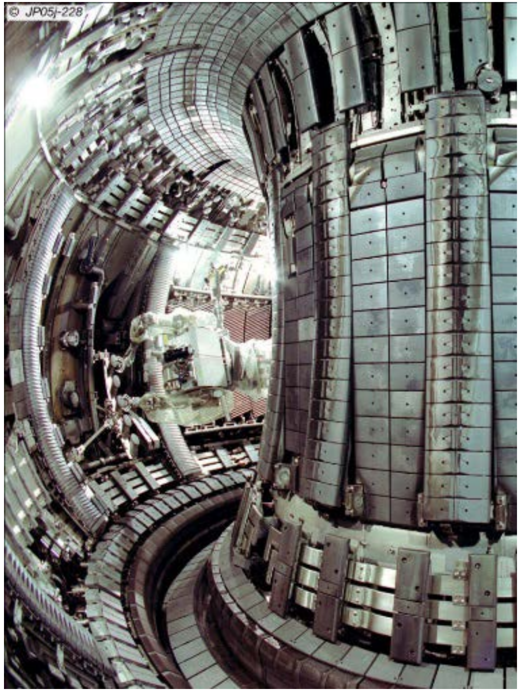

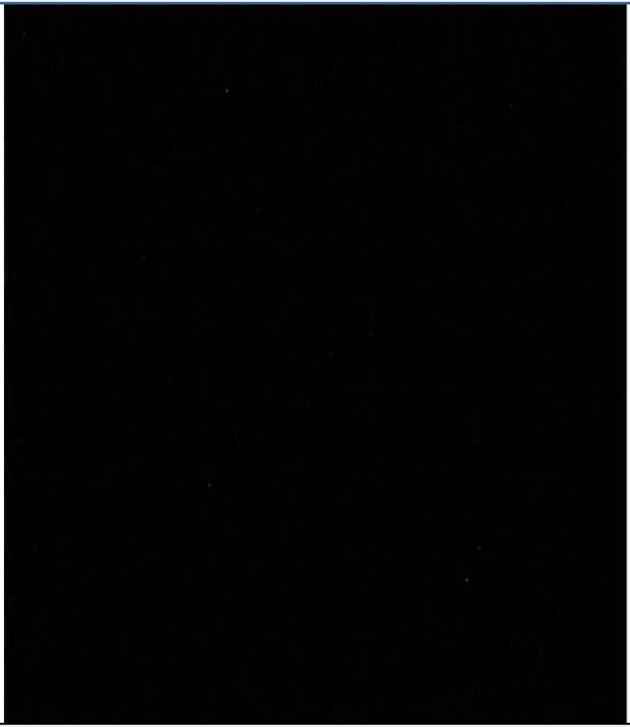

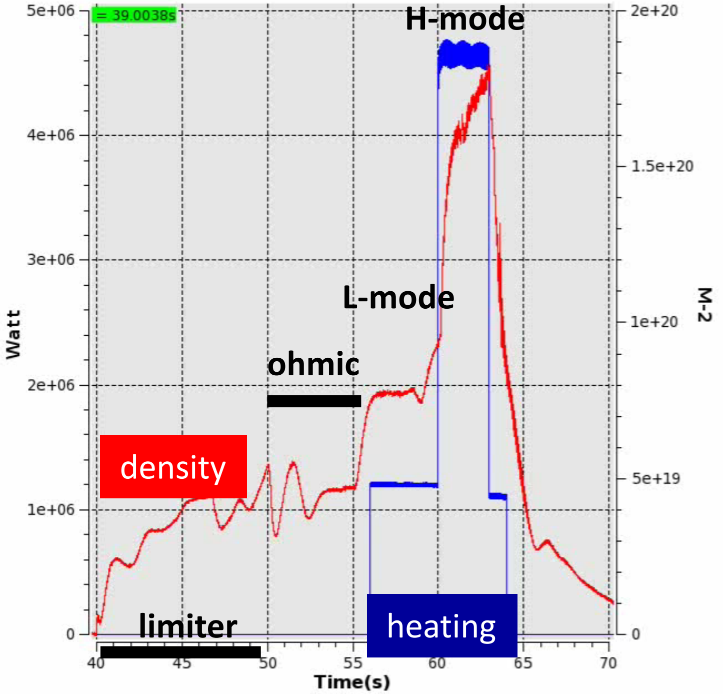

- JET plasma duration limited by available flux swing and copper coils required to induce plasma current
- Plasma discharge in different confinement modes possible: limiter, ohmic, L-mode, H-mode etc.

High Confinement Mode (H-mode)

- Transport barrier at the plasma edge (pedestal) reduces energy and particle exhaust
- Improved confinement in the confined plasma region (factor 2): basis for all scaling laws
- H-mode inherent micro-instable: release of particle to the first wall with pedestal collapse (ELMs)

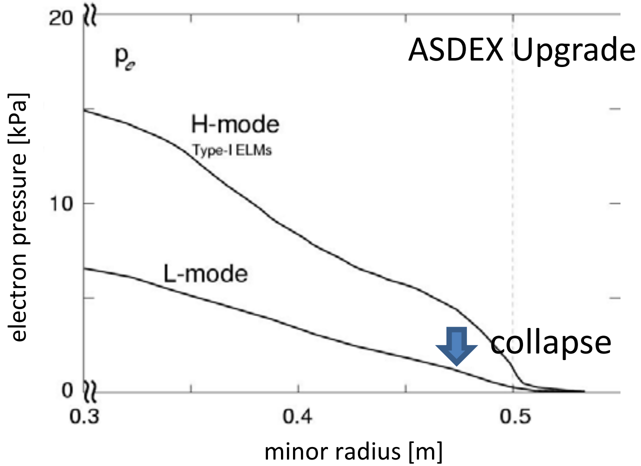

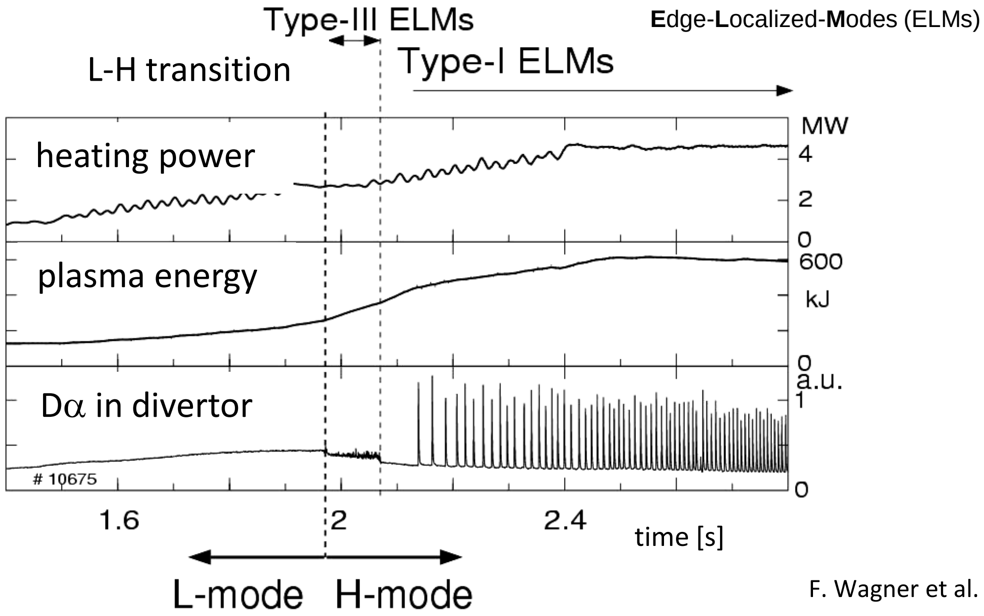

F. Wagner et al.

Spectroscopy with temporal resolution of ~1 ms in H-mode required to resolve inter and intra-ELM phases

Example of ELM Cycle Analysis in JET Divertor

- ELM averaging techniques to obtain better statistic for analysis
- Particle flux driven during ELMs and post-outgassing can induce change of local plasma
  => change from ionization to recombination dominated plasma conditions

Inner divertor | Outer divertor

Particles

Dα Photons

(recombination / opacity?)

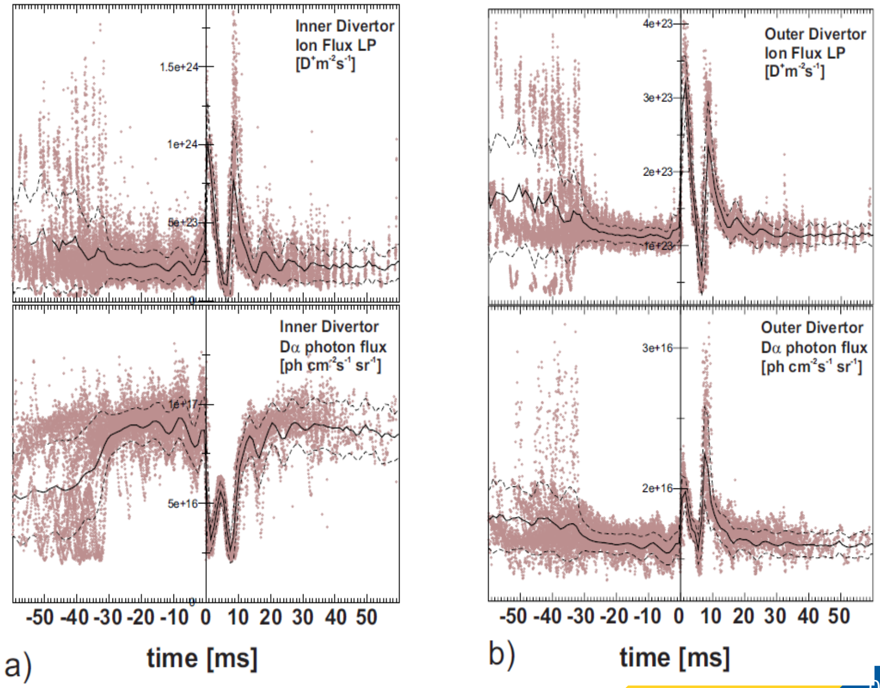

Particles

Dα Photons

(ionisation)

S. Brezinsek PS 2016

Scaling Laws: Predict the Size for a Device with τ_E=5s

Energy confinement time τ_E :

- Experimental data cannot be fully analytical described: $\tau_E \propto I_p \times R^2$
- Quality of the thermal isolation (quality of magnetic cage) determined by τ_E
- Multi-machine scaling (self-similiar H-mode plasmas) to extrapolate to required τ_E (Wind tunnel approach)
- H-mode plasmas in fully attached conditions and mostly with graphite-based PFCs

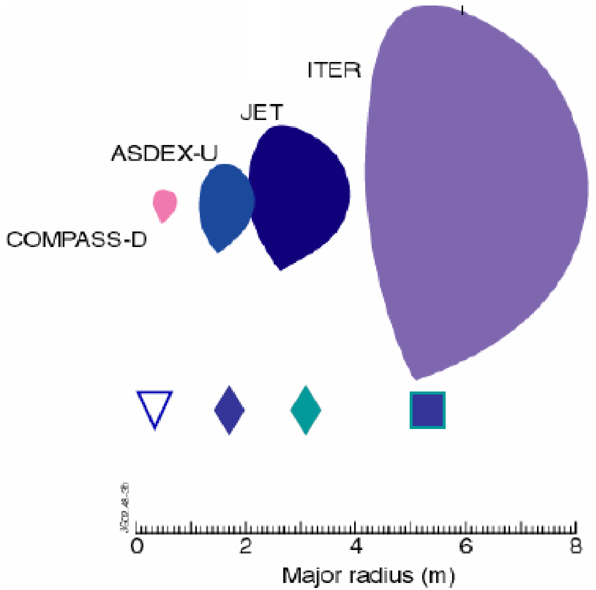

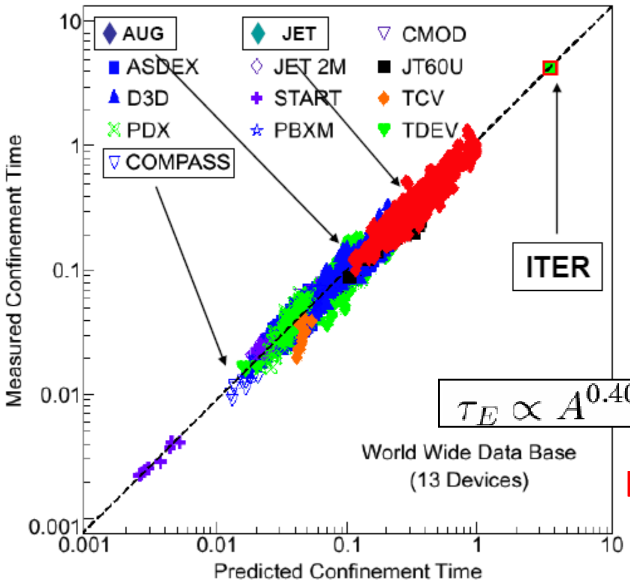

A: aspect ratio
P: input power
n: electron density
B: toroidal magnetic field
a: minor radius
n: electron density

$$\tau_E \propto A^{0.40} I^{0.90} P^{-0.65} R^{1.90} a^{0.20} \kappa^{0.80} B^{0.05} n^{0.30}$$

plasma current   major radius

Joint European Torus: JET Tokamak

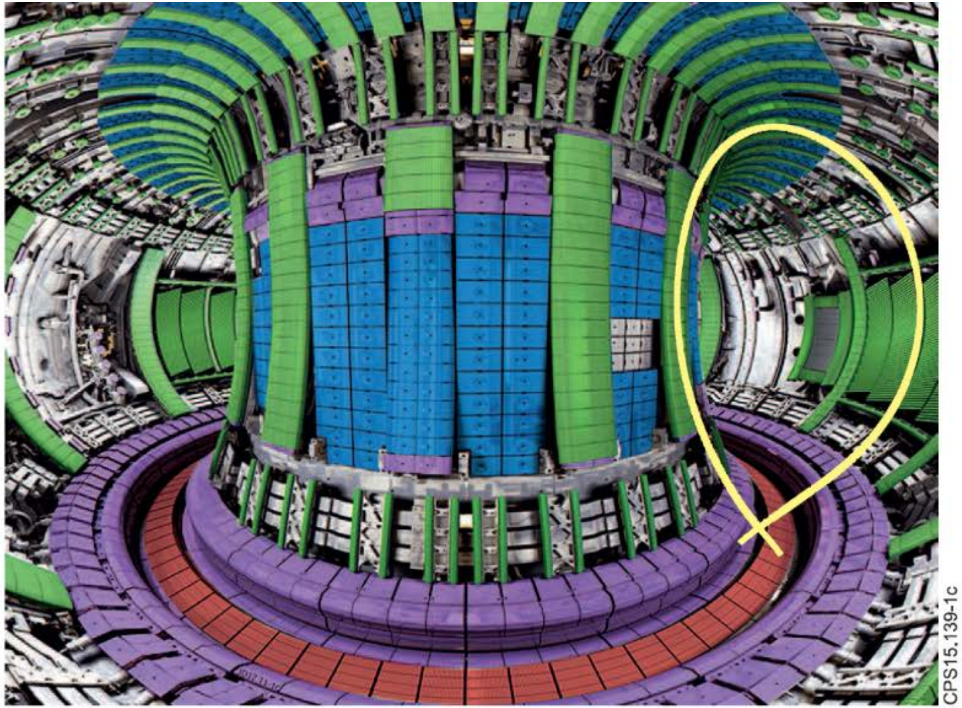

a) Bulk Be PFCs | Be–coated inconel PFCs | Bulk W | W–coated CFC PFCs

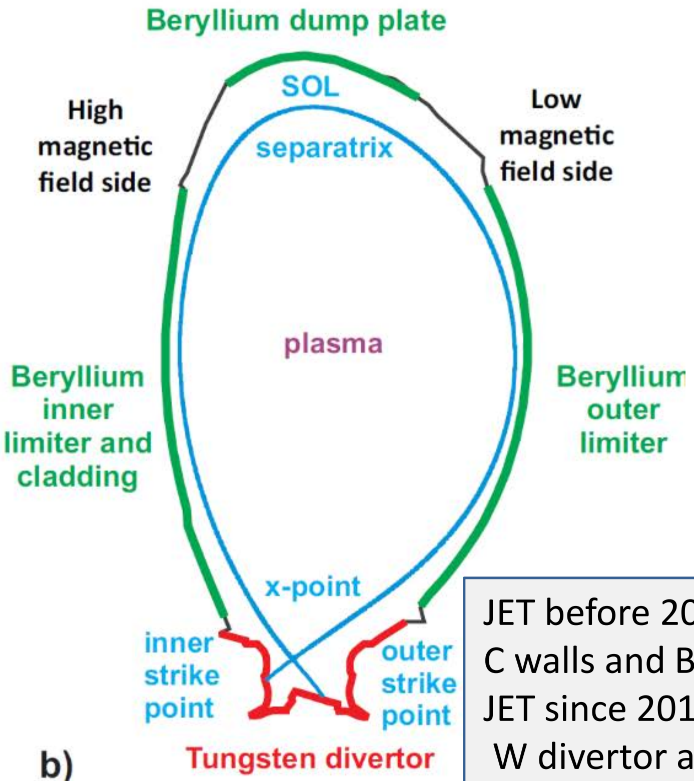

b)

JET before 2011:
C walls and Be evaporation
JET since 2012:
W divertor and Be wall

“Natural impurities” to be considered: Be, W, C as well as O (leaks) and steel components (Ni, Cr, Fe)

The Challenge with W Spectroscopy

divertor edge core

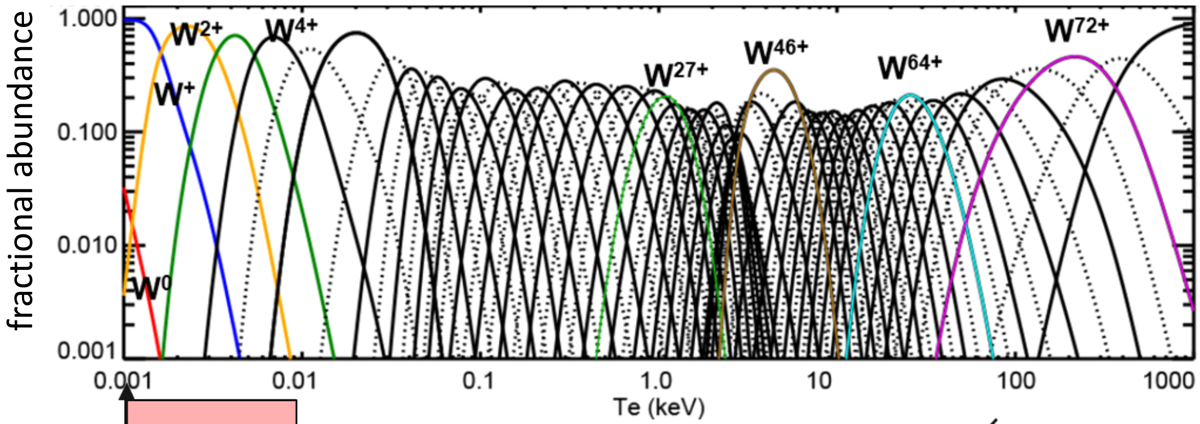

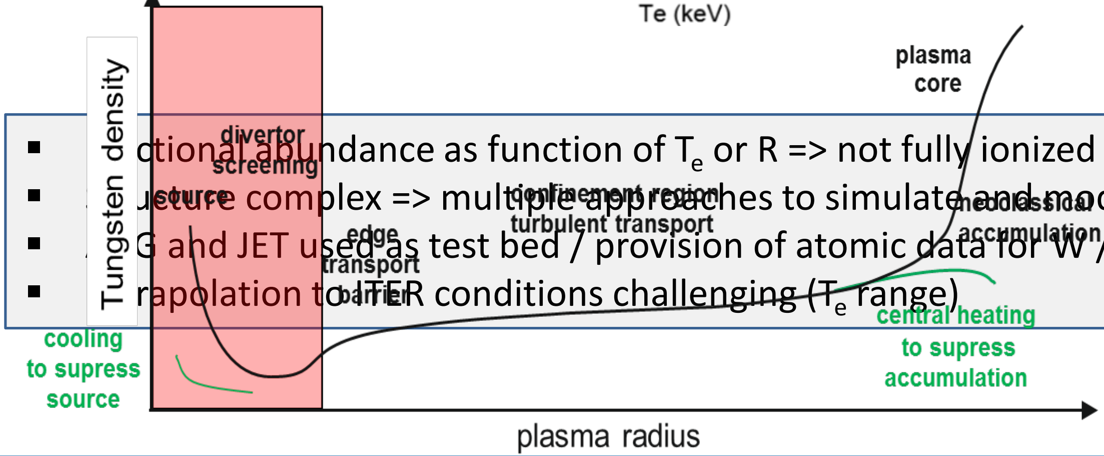

- ...ctional abundance as function of T_e or R => not fully ionized in core
- ...ucture complex => multiple approaches to simulate and model W
- A...G and JET used as test bed / provision of atomic data for W / EBIT
- ...rapolation to ITER conditions challenging (T_e range)

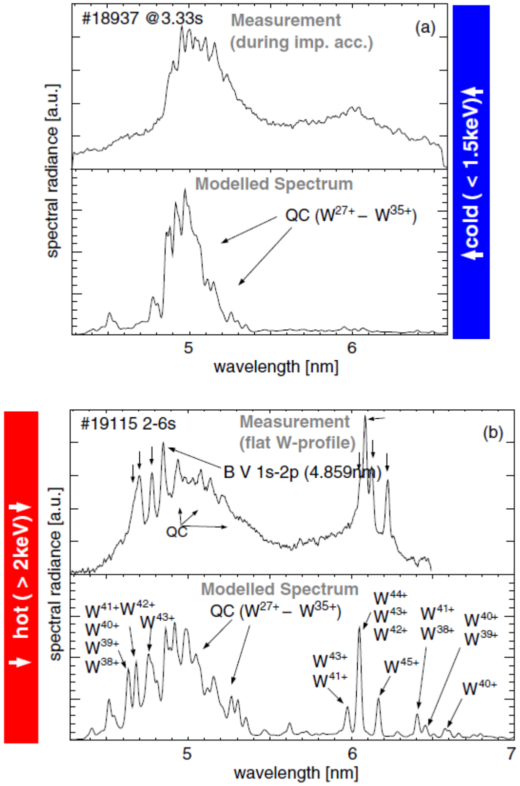

T. Pütterich PPCF 2008

The Challenge with W in Fusion Devices

- High radiation potential (core cooling)
- Prone to accumulate in core (transport)
- Low concentration is permitted (10^{-4} / 10^{-5}), but W source is small
- W control mainly via spectroscopic tools by using divertor cooling by seeding (source) and central heating (core) as actuator

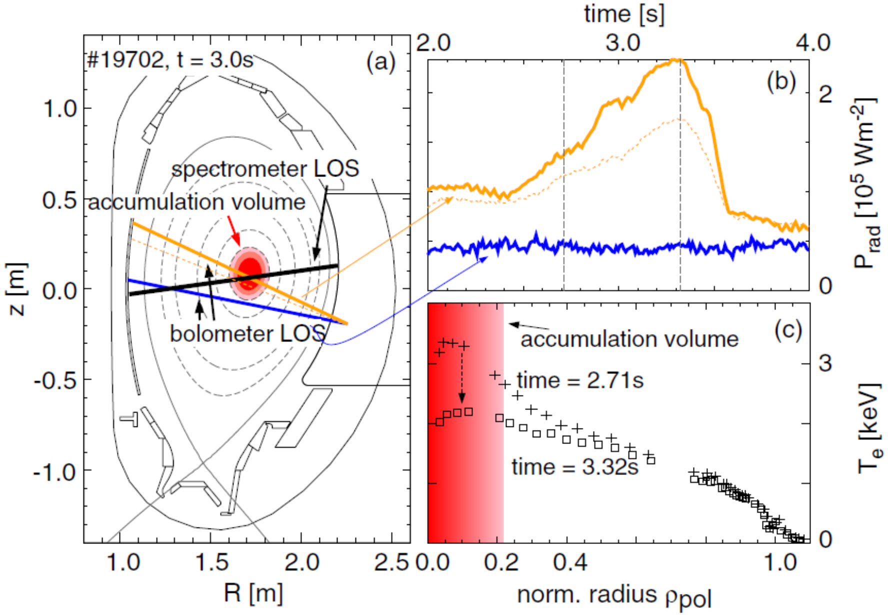

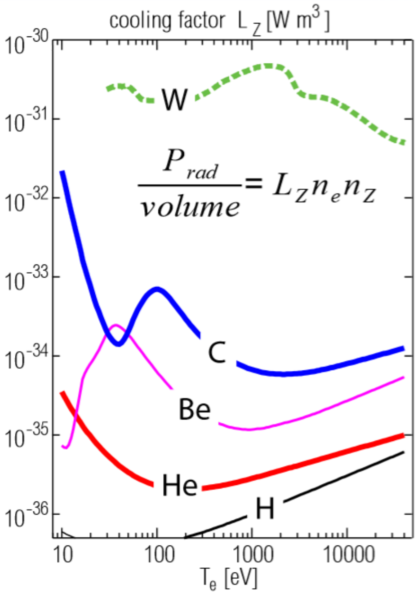

T. Pütterich PPCF 2008

Why do we bother with W?

Melting Point >2000 K
Thermal Conductivity >50 W/mK

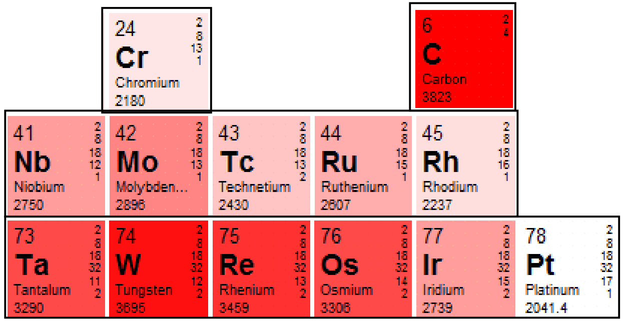

+

Availability, Cost

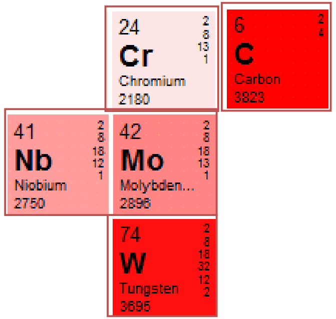

+

Low/Medium Activation

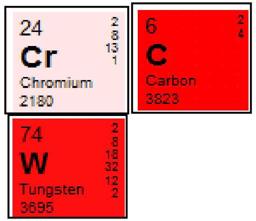

+

Erosion Retention

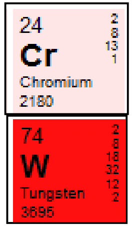

+

Temperature window (RC)

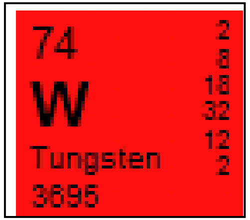

Plasma-Surface Interaction Processes

Processes depend on plasma facing material, material / projectile mass, material mix and concentration, impact energy (E_{in}), impact angle (a), roughness and temperature (T_{surf}), plasma conditions

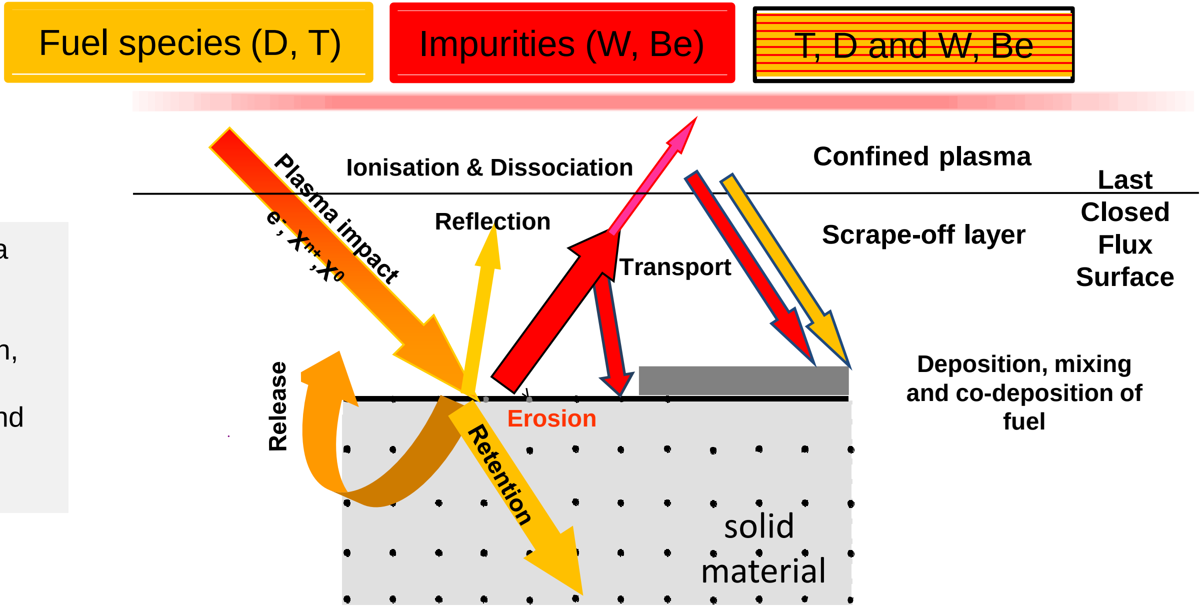

Physical Sputtering of W

- Binary-collision approximation with perpendicular impact of mono-energetic projectiles

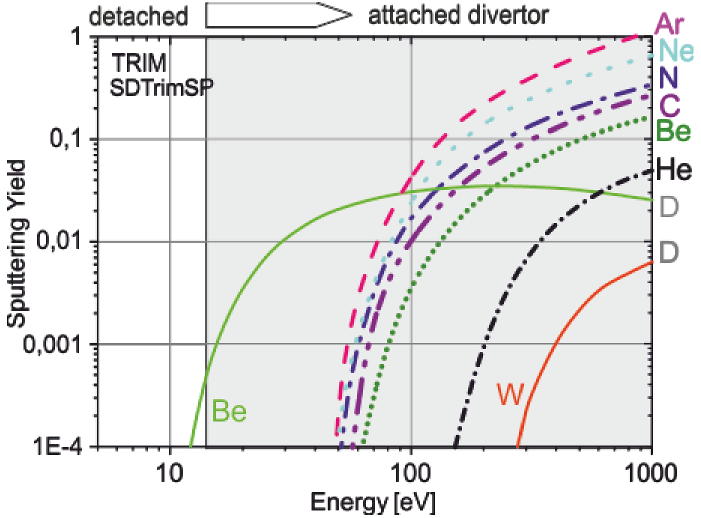

- W sputtering by intrinsic (Be, C) or seeding impurities (Ne, Ar, N) above threshold energy E_{th}
- Noticeable sputtering by D^+ above E_{in}~250eV

- Dominant in JET-ILW: Be ions ~ 0.5-1.5%

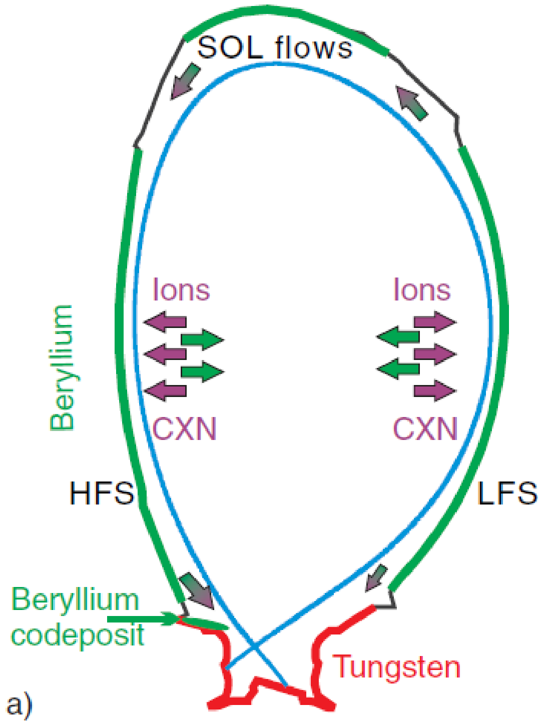

Be sources and migration in JET

S. Brezinsek NF 2015

Gross and Net Erosion of W

Optical Emission Spectroscopy (WI):
gross erosion of W [in situ]

IoniSation
Branching Ratio
EXcitation
Erosion Yield

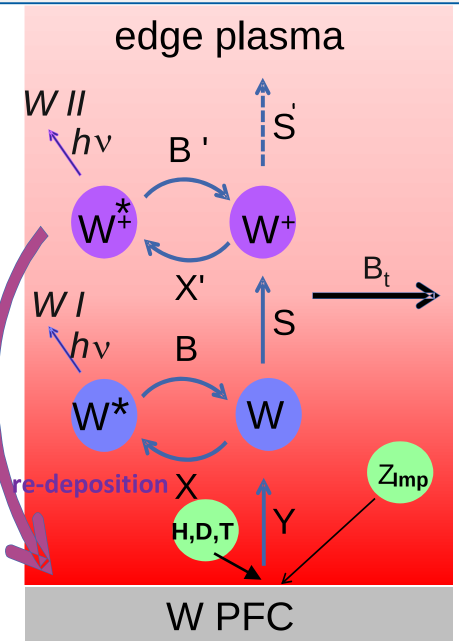

Post-Mortem Analysis Techniques:
net erosion of W [ex situ]

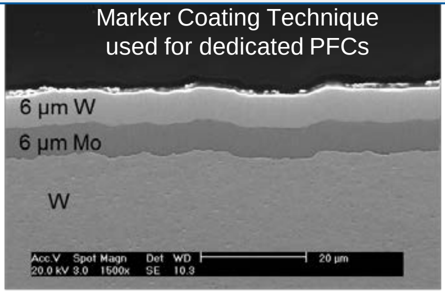

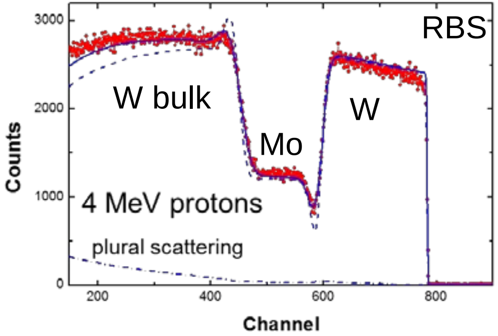

M. Mayer et al.
NME 2017

- Difference provides local W balance: eroded, re-deposited, and transported away
- Erosion of W is in general low => enough fluence to compare both methods required

Gross and Net Erosion of W

- Net W erosion at OSP measured [M. Mayer Phys. Scr. 2017]
- ~1.5µm at OSP in 900s ELMy H-mode phase

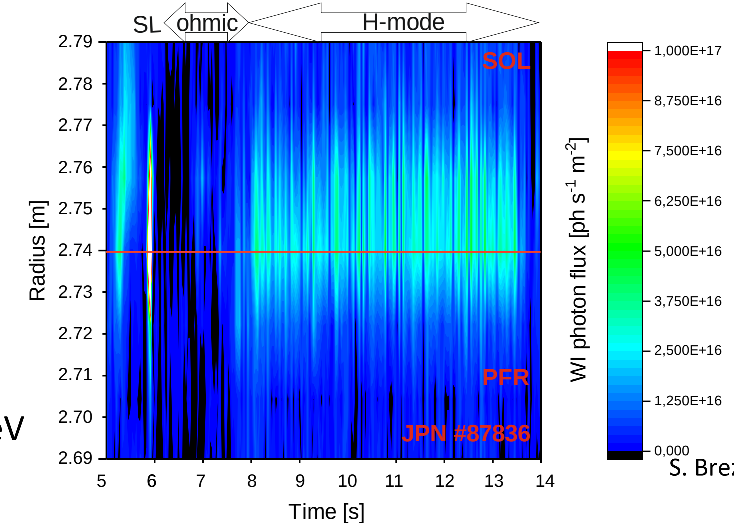

T_e=35eV

S. Brezinsek IAEA 2018

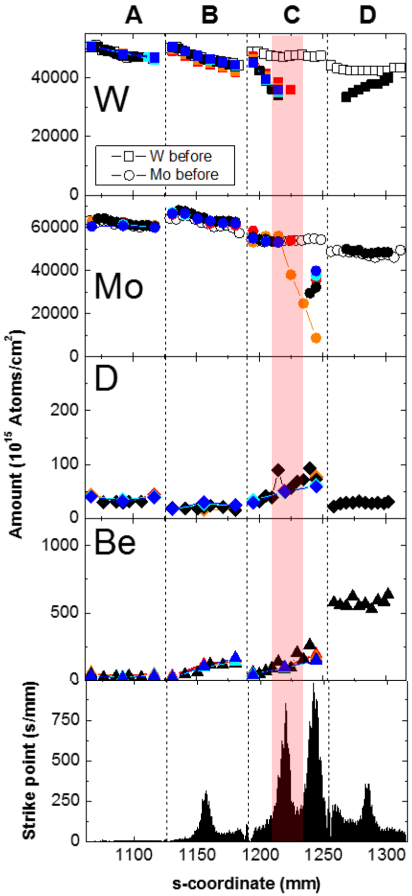

- Net W erosion: 2.4-4.8 g (RBS and marker tiles)
- Gross W erosion: 40-60 g (WI spectroscopy)
- W re-deposition fraction: >92%

Prompt Redeposition: a High-Z (Tungsten) Effect

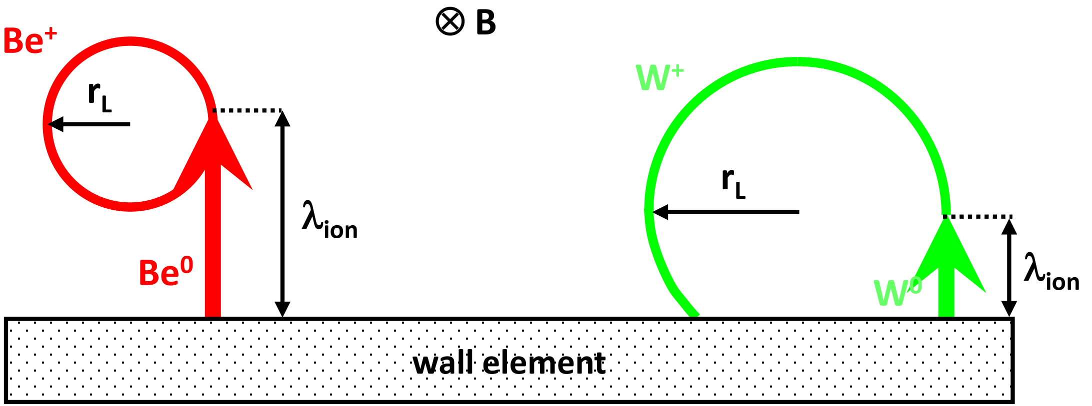

W I and W II spectroscopy ?

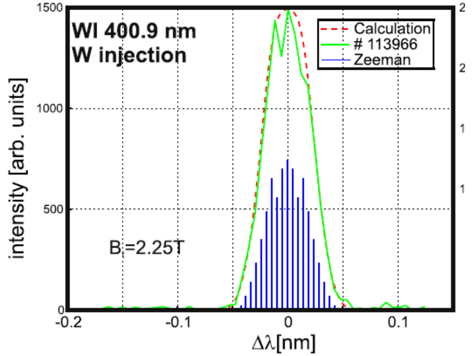

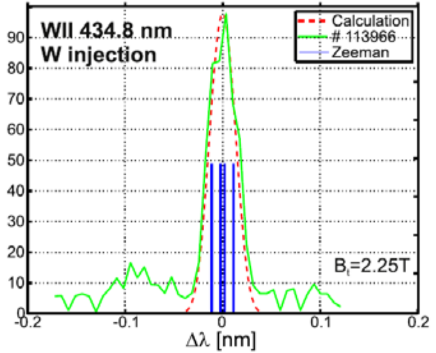

Larmor radius: $r_L = M \cdot v_\perp / q \cdot B$

Ionisation length: $\lambda_{ion} = v_\perp / \langle\sigma v\rangle_{ion} \cdot n_e$

$$\rho_{prompt} = \lambda_{ion} / r_L$$

- Prompt redeposition if $\rho_{prompt} < 1$ $\Rightarrow$ large mass and large ionisation probability
- Results in LOW net erosion for W if prompt re-deposition is high.

ELM-induced W Sputtering in Detached Conditions

Inter-ELM W source can be eliminated when divertor is semi-detached and impact energies below the threshold for impurities

Intra-ELM W source can burn through the cushion of hydrogen and seeding neutrals

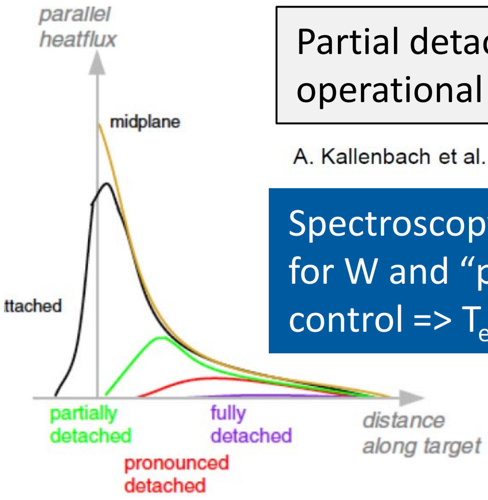

Partial detachment is the operational regime for ITER

A. Kallenbach et al.

Spectroscopy often used for W and "power" control => T_e sensitivity

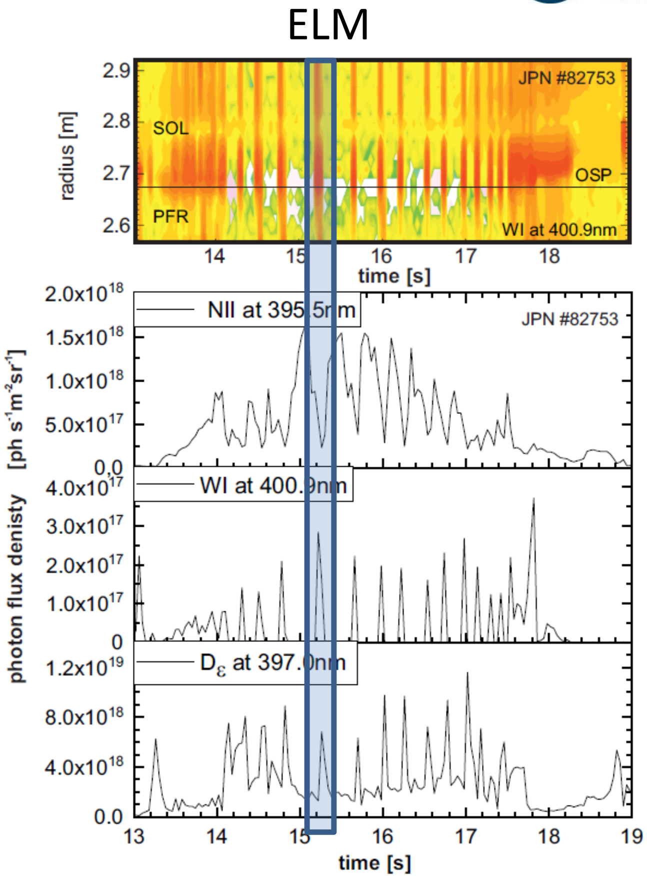

Ionisation and Recombination

Usage of Balmer lines or NII lines (seeding) to locate ionization front

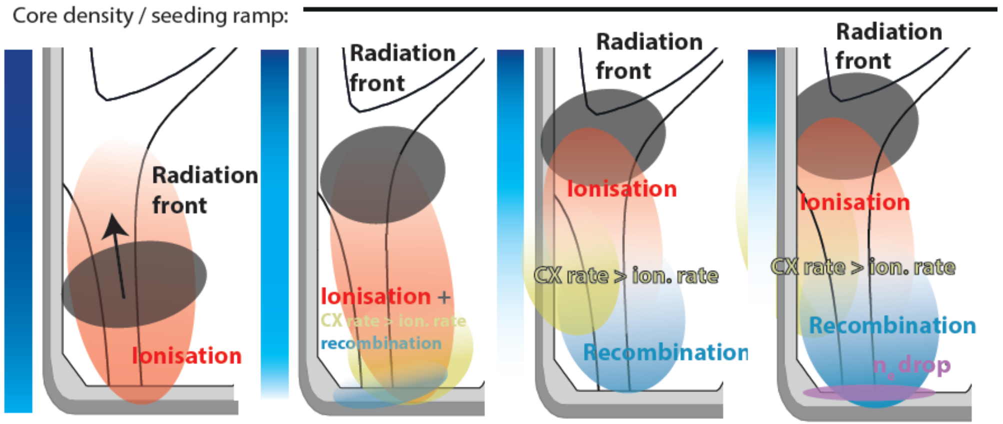

K. Verhaegh (TCV)

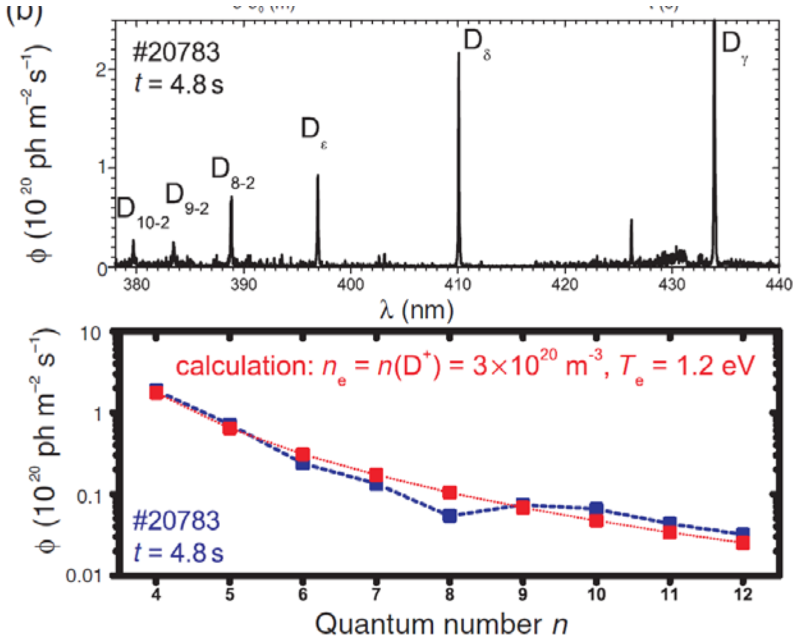

Plasma conditions determined by e.g. line ratios and appropriate CRMs (e.g. YACORA)

The Power and Particle Exhaust Issue for ITER

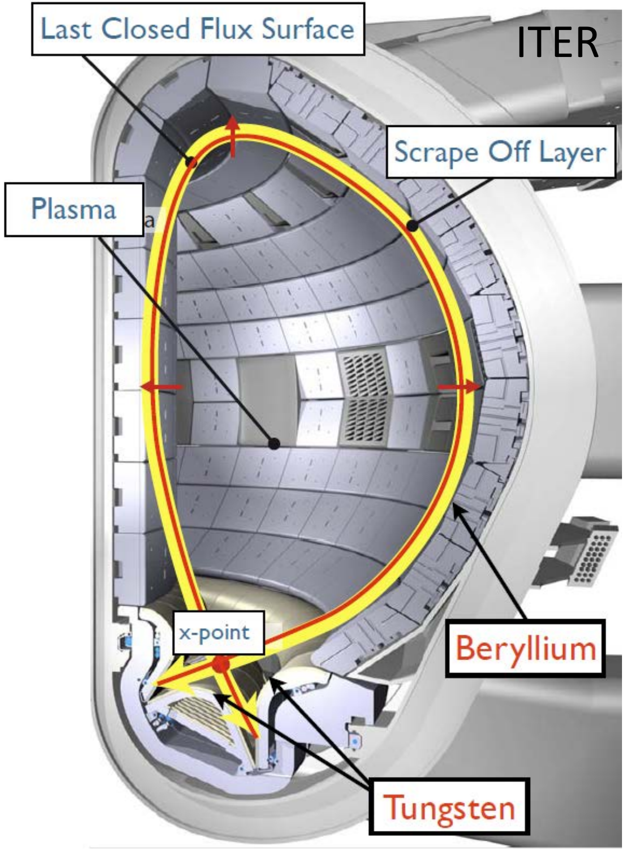

- In order to meet the burning conditions, a certain machine size and auxiliary power topped-up by α-heating
- Neutrons transport 80% of the energy to the wall and blanket modules: heat load on the wall
- He-ash (residual from α heating) is transported out of the plasma on a faster timescale than the energy confinement time
- Particles (D^+, T^+, He^{2+}, e^-) are transported in the scrape-off layer towards the divertor target plates at glancing incidence
- In the original scaling law for ITER (unfueled H-mode with 500MW=P_{fus}) one reaches at the target plates more than 40 MW/m^2
- In order to meet limits of materials / components (10MW/m^2) one needs to ADAPT the plasma solution by strong divertor radiation
- To enable DT plasma operation: W concentration needs to be below 10^{-4} which also is connected to life time issues via erosion

Step Ladder Approach to a Nuclear Fusion Reactor

Worldwide approach for a reactor based on a METALLIC tokamak concept

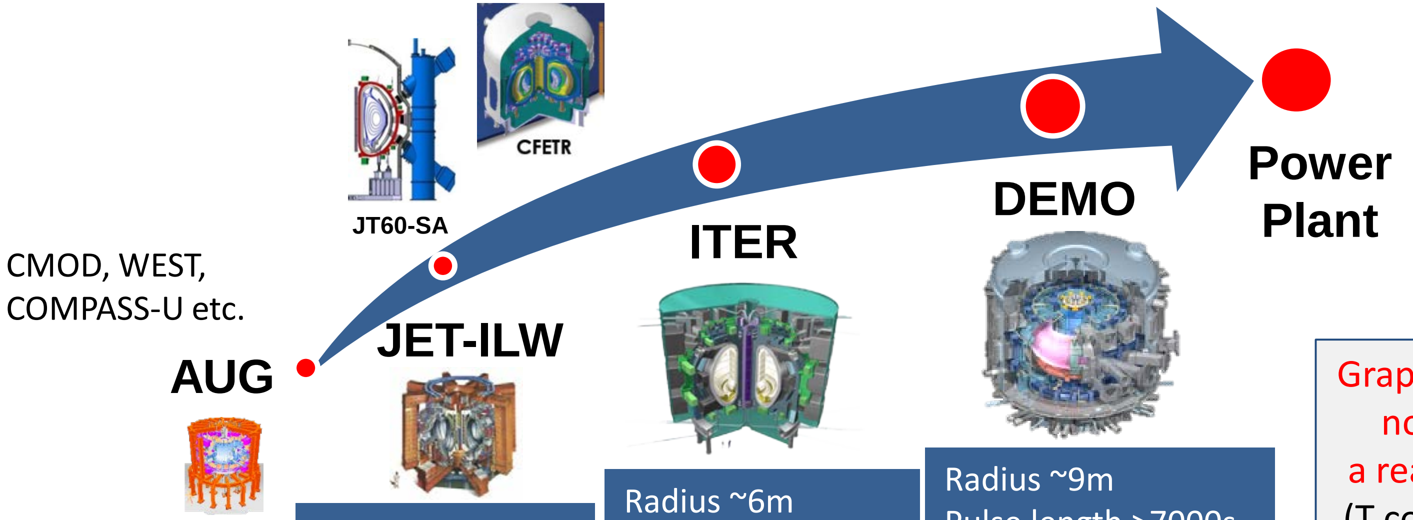

AUG
Radius ~1.6m
Pulse length ~10s

Tungsten wall
Tungsten divertor

JET-ILW
Radius ~3m
Pulse length ~15s

Beryllium wall
Tungsten divertor

ITER
Radius ~6m
Pulse length ~400s
P_{fusion} ~0.5GW

Beryllium wall
Tungsten divertor

DEMO
Radius ~9m
Pulse length >7000s
P_{fusion} ~2.0 GW

Steel wall (EUROFER)
Tungsten divertor

Graphite PFCs presently not considered for a reactor due to safety (T co-deposition, dust), lifetime (C erosion), and tritium cycle (T retention) issues!

Next Step Device: ITER

International Thermonuclear Experimental Reactor

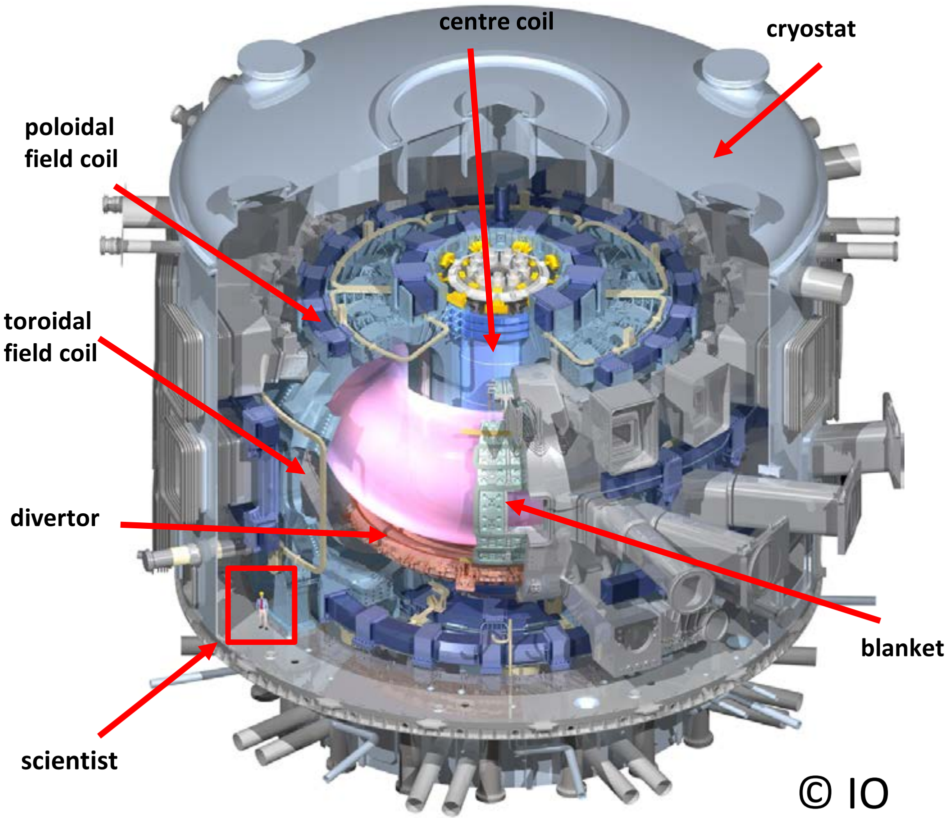

- To demonstrate (i) scientific and (ii) technical /plasma-surface interaction feasibility of fusion
- To achieve extended burn in inductively-driven DT plasma operation with Q=10 (400s)
- To demonstrate readiness of essential fusion technologies (incl. plasma-facing components)
- To test tritium breeding module concepts with 14 MeV-neutron power load on the first wall

Major Radius: 6.2 m
Minor Radius: 2.0 m
Plasma volume: 840 m^3
Surface area: 260m^2 W and 620m^2 Be
Plasma current: 15 MA
Magnetic field: 5.3 T (12 T)
Energy content: 350 MJ
Auxiliary heating: 70-100 MW
Height: ~25 m and Diameter: ~26 m

ITER Timeline

Step-wise construction of the tokamak and accompanied exploration program

limiter
plasma (H)

PFPO
divertor plasma (H, He)

FPO
divertor plasma (D, DT)

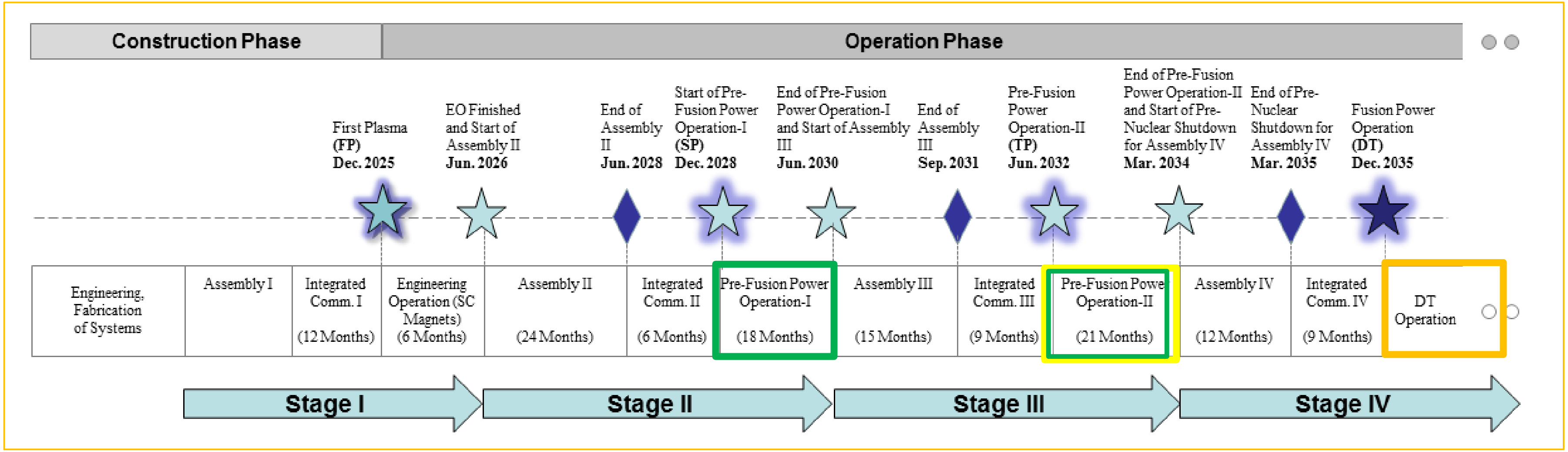

- Large number of spectroscopic systems in support and simulation
- Variation in spectroscopic sensitivity from low power to high power discharges
- ITER requires in addition seeding species: Ne, N_2, Kr as seeding gas + Ar for DMS

ITER research plan (2018)
https://www.iter.org/technical-reports

ITER Tokamak

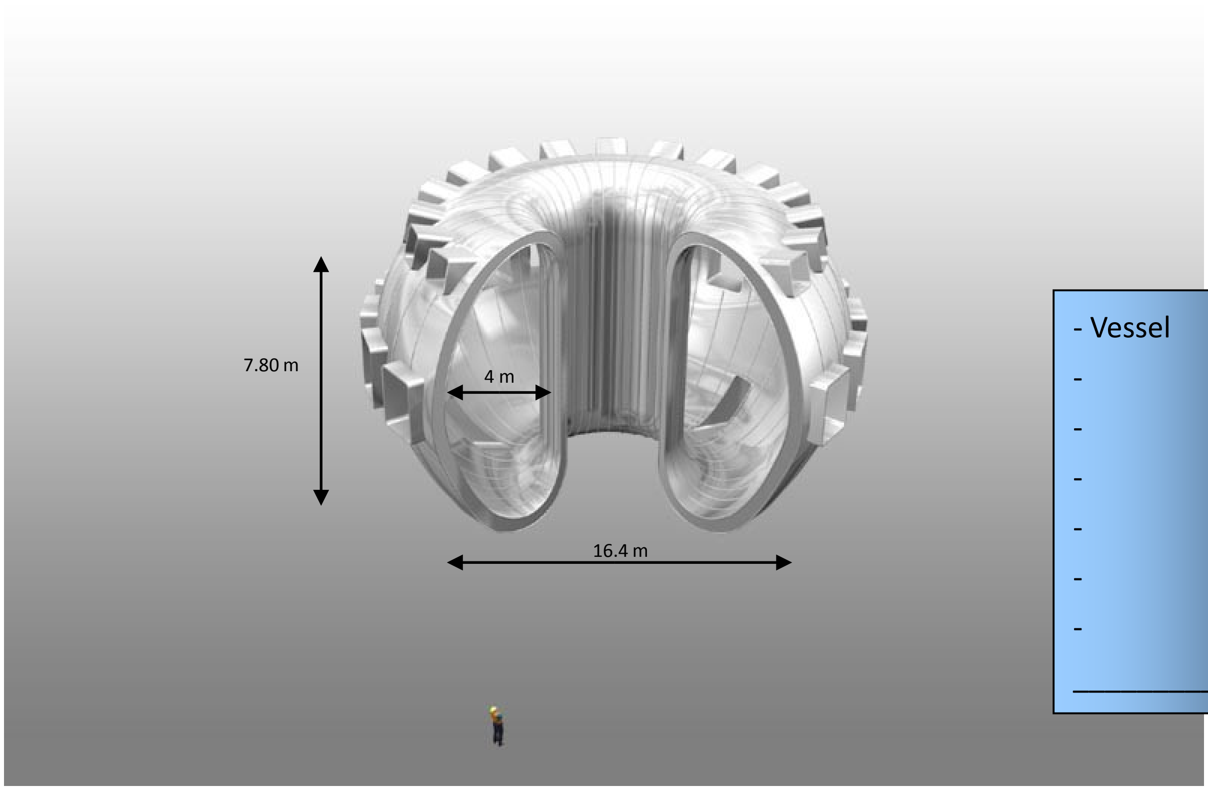

- Vessel
-
-
-
-
-
-

____

ITER Tokamak

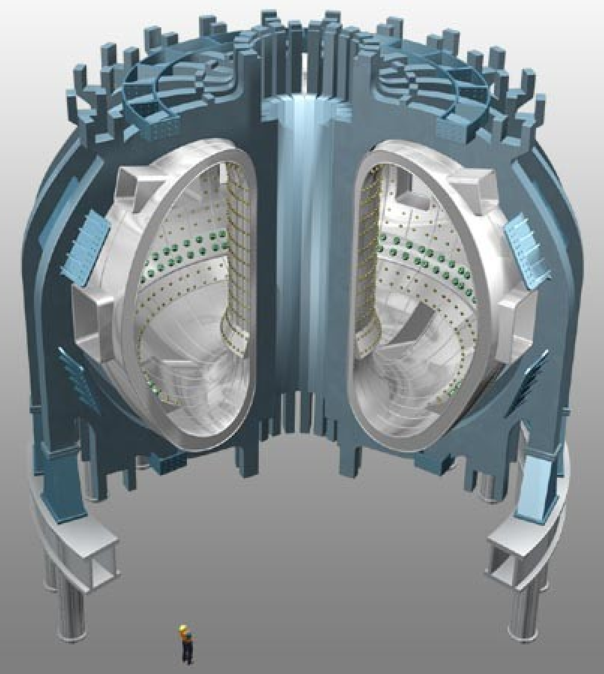

18 coils
superconducting

5.3 T

8 700 to

- Vessel
- Toroidal Coils
-
-
-
-
-

____

© IO

ITER Tokamak

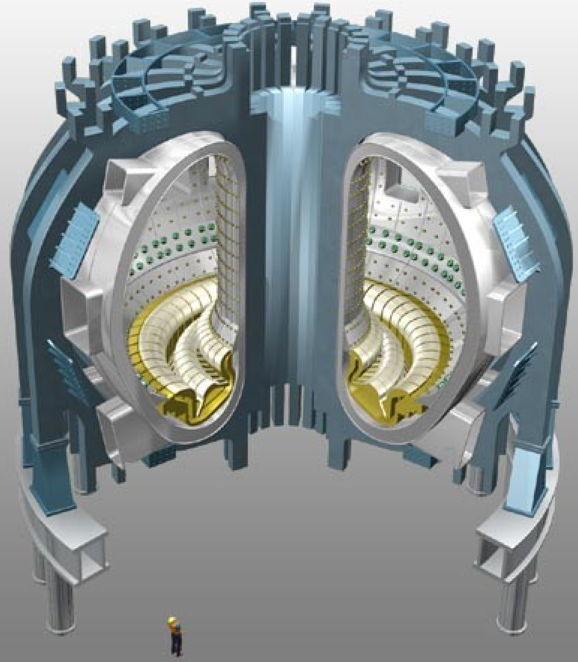

10 MW / m^2 on 8 m^2

- Vessel
- Toroidal Coils
- Divertor
-
-
-
-

___

ITER Tokamak

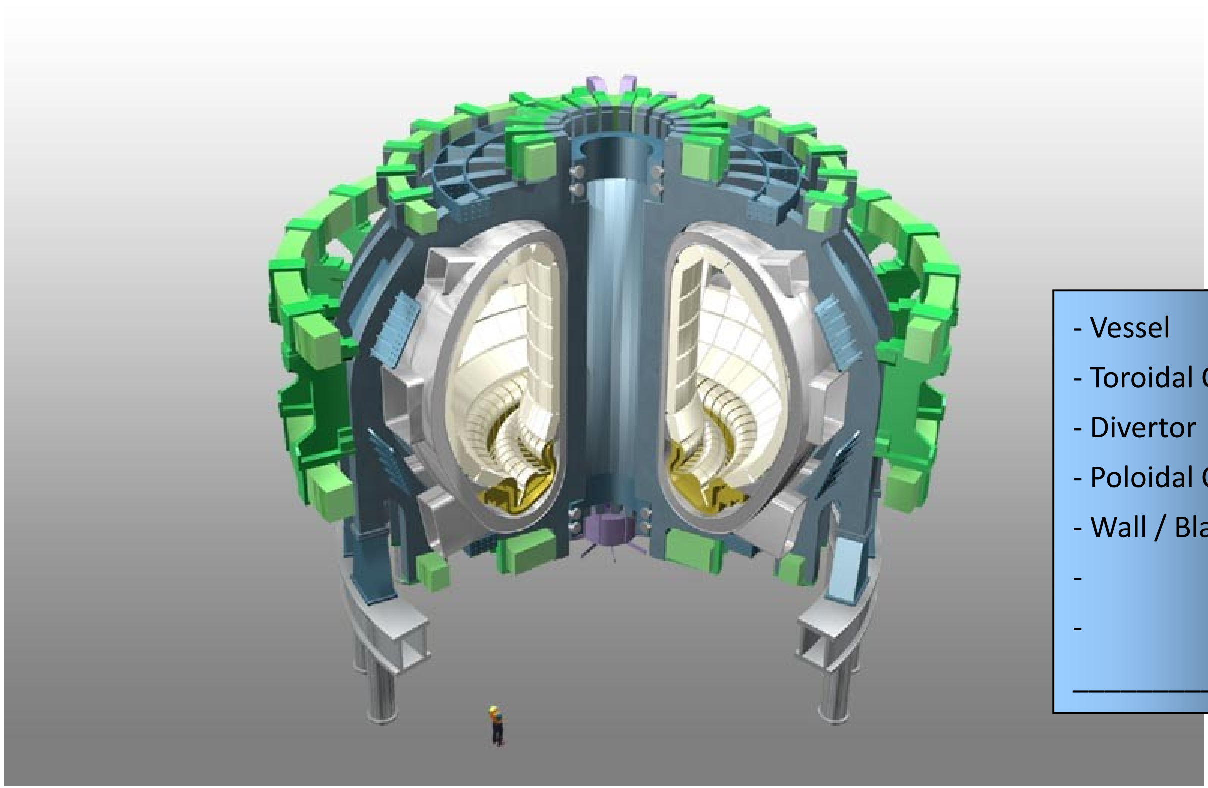

- Vessel
- Toroidal Coils
- Divertor
- Poloidal Coils
- Wall / Blanket
-
-

____

ITER Tokamak

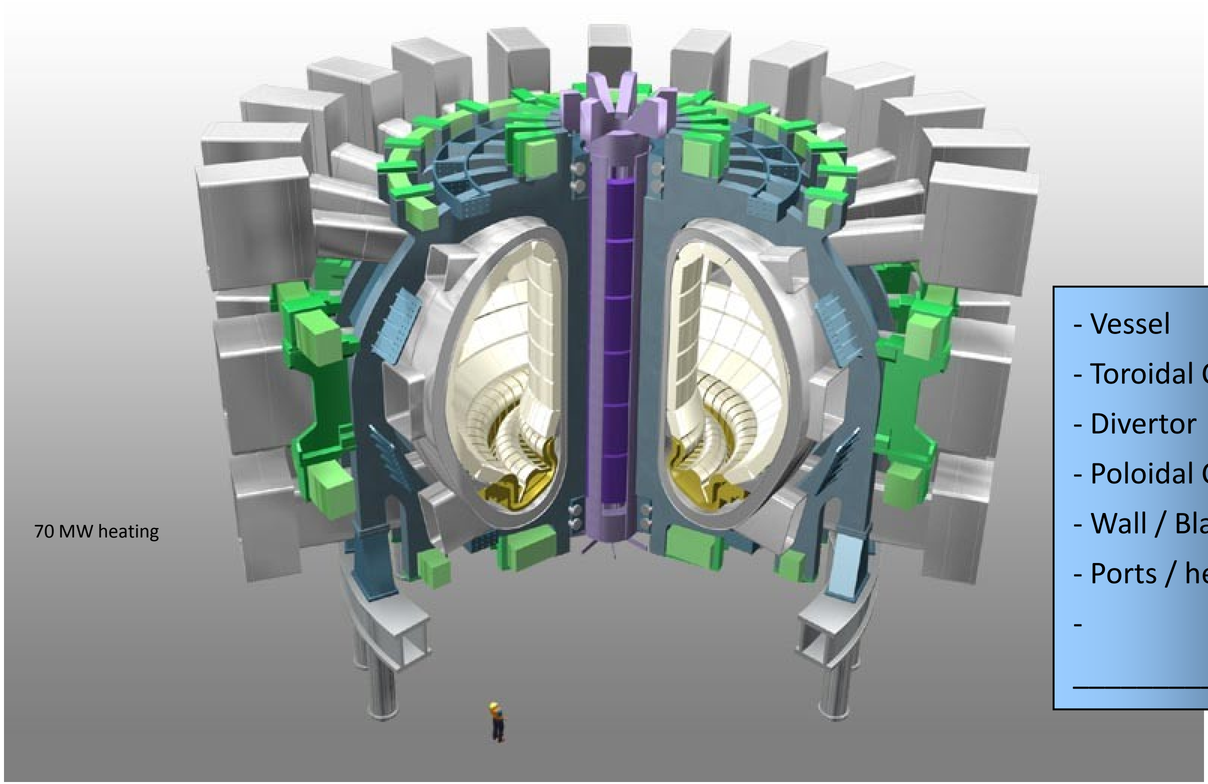

- Vessel
- Toroidal Coils
- Divertor
- Poloidal Coils
- Wall / Blanket
- Ports / heating
-

____

ITER Tokamak

-Diagnostics
- Tritium Plant
- Remote Handling
- Control & Data
____

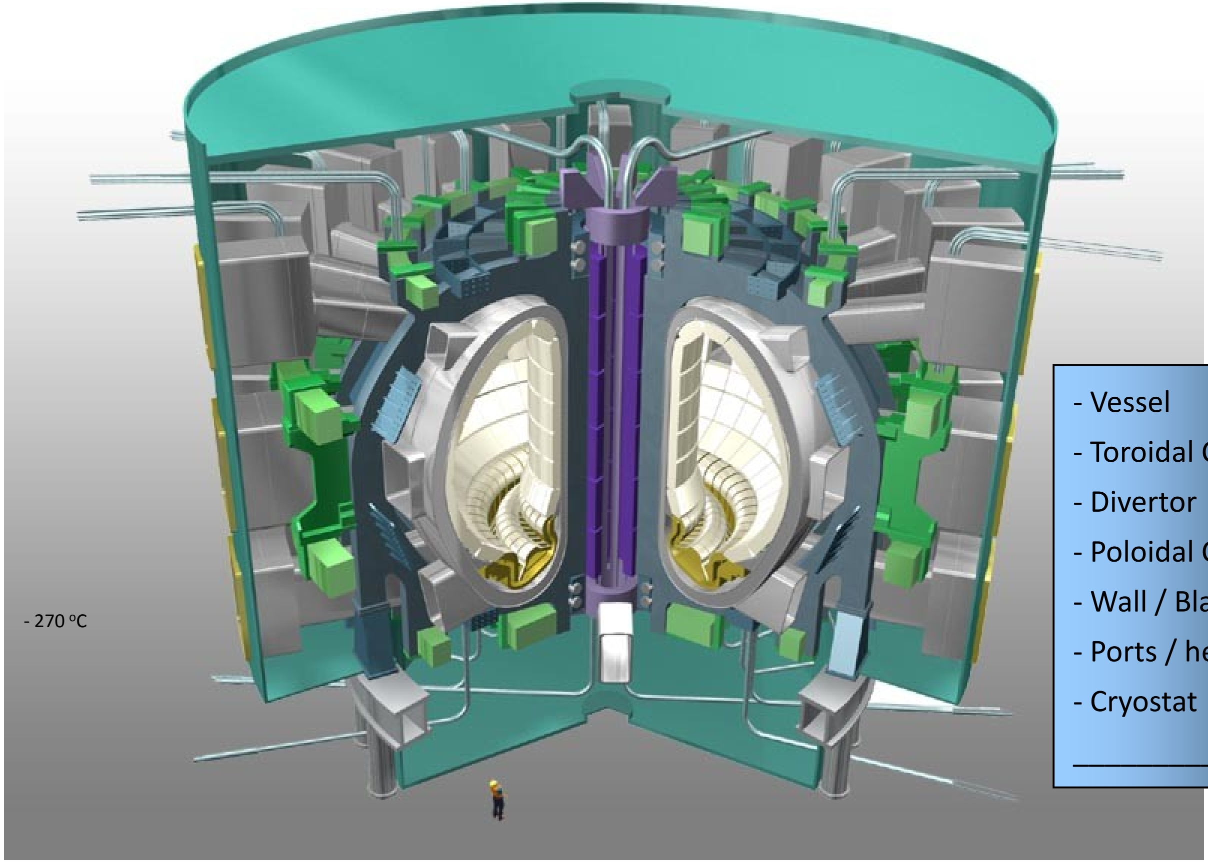

- Vessel
- Toroidal Coils
- Divertor
- Poloidal Coils
- Wall / Blanket
- Ports / heating
- Cryostat

____

Tokamak Complex in Cadarache

© IO

Resting on 493 seismic pads, the 440 000-ton Tokamak Complex comprises 7 levels (2 underground).

ITER: Tokamak Building and Infrastructure

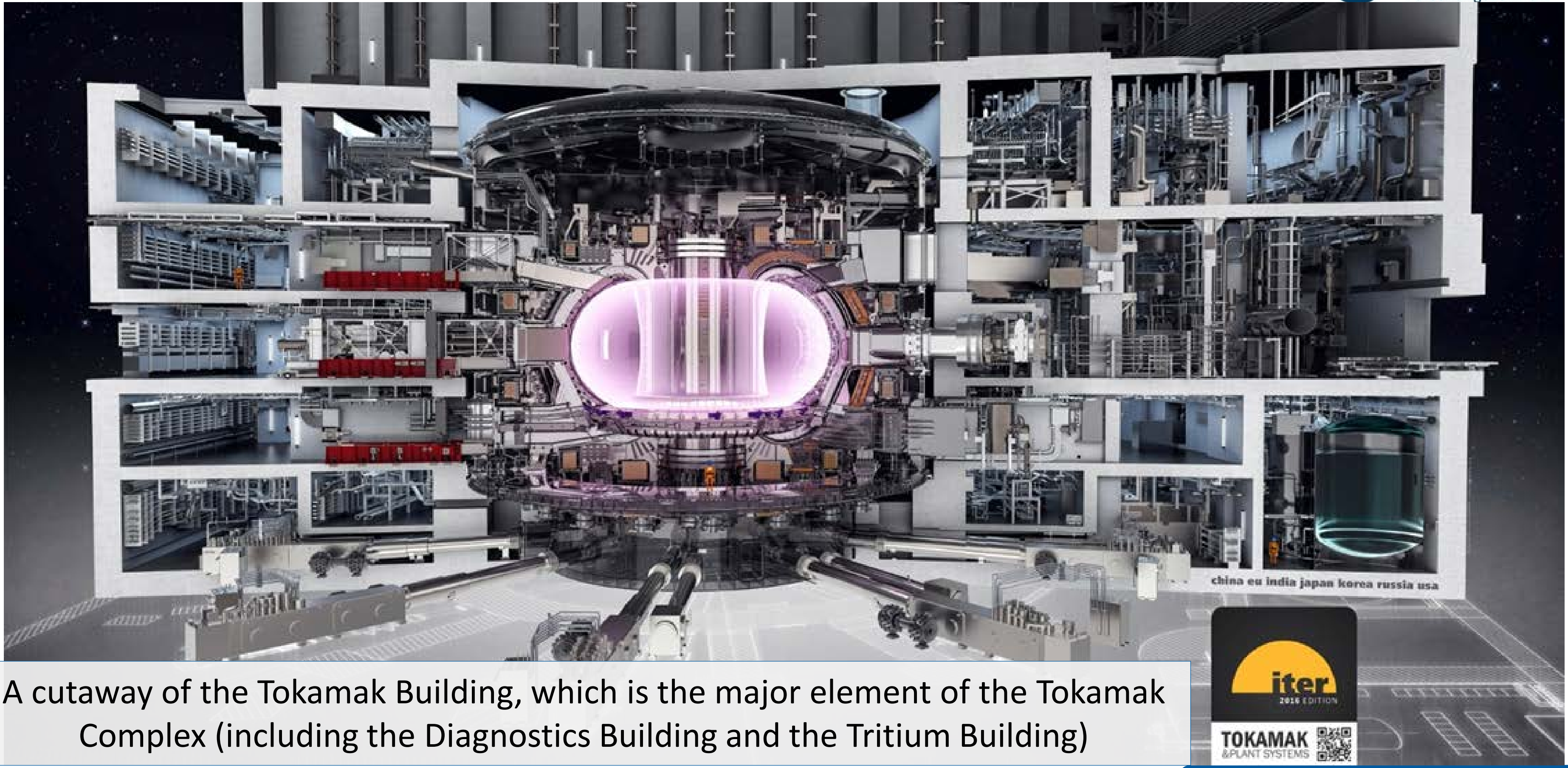

A cutaway of the Tokamak Building, which is the major element of the Tokamak Complex (including the Diagnostics Building and the Tritium Building)

Diagnostic Building

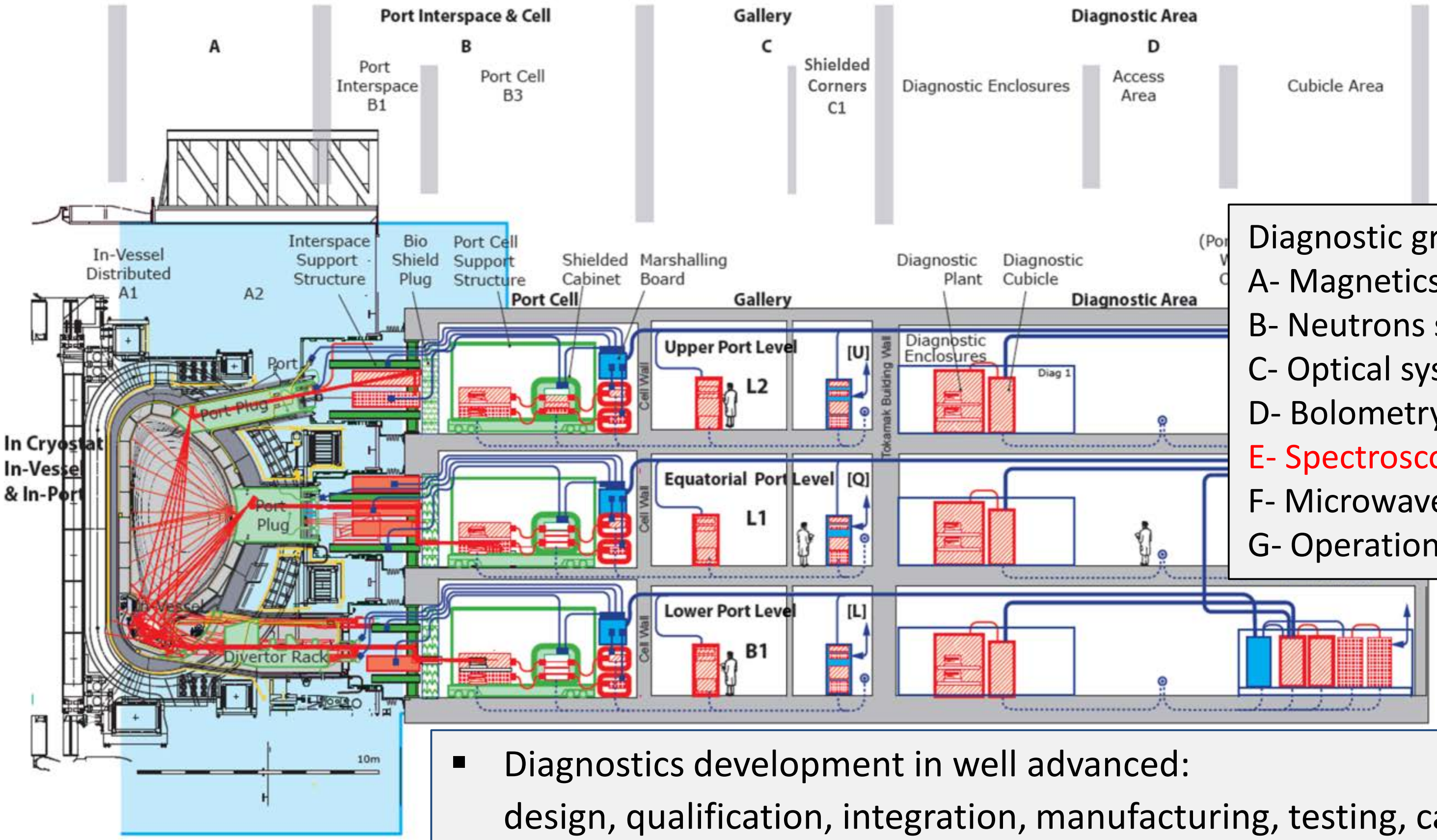

Diagnostic grouping
A- Magnetics systems
B- Neutrons systems
C- Optical systems
D- Bolometry systems
E- Spectroscopy systems
F- Microwave systems
G- Operational systems

R. Barnsley et al.

- Diagnostics development in well advanced:
  design, qualification, integration, manufacturing, testing, cabling

Spectroscopic Diagnostics in ITER and their Purpose

PBS	System	Range	Function	PA	Status
55E4	Divertor imp monitor	200 – 1000 nm	Impurity species and influx, divertor He density, ionisation front position, T_i.	Yes	PDR prep
55E2	Ha system	Visible region	ELMs, L/H mode indicator, n_T/n_D and n_H/n_D at edge and in divertor.	Yes	PDR held
55E3	VUV spectr. – main	2.3 – 160 nm	Impurity species identification.	Yes	**PDR held**
55EG	VUV spectr. – divertor	15 – 40 nm	Divertor impurity influxes, particularly Tungsten	Yes	**PDR held**
55EH	VUV spectr. – edge	15 - 40 nm	Edge impurity profiles	Yes	**PDR held**
55ED	X-ray spectr. – survey	0.1 – 10 nm	Impurity species identification	Yes	PDR prep
55EI	X-ray spectr. – edge	0.4 – 0.6 nm	Impurity species identification, plasma rotation, T_i.	Yes	PDR prep
55E5	X-ray spectr.-core	0.1 – 0.5 nm		Yes	PDR prep
55E7	Radial x-ray camera	1 – 200 keV	MHD, Impurity influxes, Te	Yes	PDR held
55EB	MSE	Visible region	q (r), internal magnetic structure	Yes	PDR prep
55E1	Core CXRS	Visible region	T_i (r), He ash density, impurity density profile, plasma rotation, alphas.	No	**CDR held**
55EC	Edge CXRS	Visible region		Yes	PDR prep
55EF	Pedestal CXRS	Visible region	Best spatial resolution of H-mode pedestal	No	CDR held
55E8	NPA	0.01- 4 MeV	n_T/n_D and n_H/n_D at edge and core. Fast alphas.	Yes	PDR closed
55EA	LIF	Visible	Divertor neutrals	No	Pre- CDR held
55E	Hard X-ray Monitor	100keV – 20MeV	Runaway electron detection	IO	PDR prep

passive spectroscopy

active (NBI) spectroscopy

active (LASER) spectroscopy

R. Barnsley et al.

R. Barnsley et al.

ITER Plasma Diagnostics

=> Spectrocopy

Spectroscopic Diagnostics in ITER and their Purpose

JÜLICH Forschungszentrum

PBS	System	Range	Function	PA	Status
55E4	Divertor imp monitor	200 – 1000 nm	Impurity species and influx, divertor He density, ionisation front position, T_i.	Yes	PDR prep
55E2	Ha system	Visible region	ELMs, L/H mode indicator, n_T/n_D and n_H/n_D at edge and in divertor.	Yes	PDR held
55E3	VUV spectr. – main	2.3 – 160 nm	Impurity species identification.	Yes	**PDR held**
55EG	VUV spectr. – divertor	15 – 40 nm	Divertor impurity influxes, particularly Tungsten	Yes	**PDR held**
55EH	VUV spectr. – edge	15 - 40 nm	Edge impurity profiles	Yes	**PDR held**
55ED	X-ray spectr. – survey	0.1 – 10 nm	Impurity species identification	Yes	PDR prep
55EI	X-ray spectr. – edge	0.4 – 0.6 nm	Impurity species identification, plasma rotation, T_i.	Yes	PDR prep
55E5	X-ray spectr.-core	0.1 – 0.5 nm		Yes	PDR prep
55E7	Radial x-ray camera	1 – 200 keV	MHD, Impurity influxes, Te	Yes	PDR held
55EB	MSE	Visible region	q (r), internal magnetic structure	Yes	PDR prep
55E1	Core CXRS	Visible region	T_i (r), He ash density, impurity density profile, plasma rotation, alphas.	No	**CDR held**
55EC	Edge CXRS	Visible region		Yes	PDR prep
55EF	Pedestal CXRS	Visible region	Best spatial resolution of H-mode pedestal	No	CDR held
55E8	NPA	0.01- 4 MeV	n_T/n_D and n_H/n_D at edge and core. Fast alphas.	Yes	PDR closed
55EA	LIF	Visible	Divertor neutrals	No	Pre- CDR held
55E	Hard X-ray Monitor	100keV – 20MeV	Runaway electron detection	IO	PDR prep

passive spectroscopy

active (NBI) spectroscopy

active (LASER) spectroscopy

R. Barnsley et al.

R. Barnsley et al.

Emission Bands and Systems Components

	X-ray	VUV	Visible
Typical plasma region	Core plasma	Outer plasma	Edge and divertor
Wavelength	0.1 – 10 nm	2 – 200 nm	300-800 nm
Input optics	Direct views	Grazing incidence mirrors	Normal incidence mirrors
Windows	Polymer and Beryllium windows	Not possible Requires vacuum extension	Glass, quartz etc
Dispersion	Crystal or pulse-height	Grating	Grating
Detectors	CCD, Active Pixel Photon counting	Channel-plate, CCD	CCD, CMOS

R. Barnsley et al.

Specific Issue in Nuclear Enviroment: Radiation

- Diagnostics need to be optimized regarding neutron flux and fluence impact:
  - Shielding, distance or not sensitive to neutrons

Location	Neutron flux /cm^2.s	Suitable technology	Issues
Plasma - facing	~10^{14}	Metal mirrors Retro-reflectors Waveguides	Deposition and erosion by plasma. Maintenance: - possible if in-port - remote handling if in-vessel
In-vessel Behind blanket	~10^{12}	Mineral-insulated cable Pick-up coils for magnetics	Radiation induced, EMF, currents, insulation breakdown Maintenance almost impossible
Inside port-plug	~10^8 - 10^{12}	Mirrors Replaceable detectors	Some maintenance possible
Behind port-plug	< ~10^8	Optical fibres, lenses, CCD detectors, conventional electronics. “Almost anything”	Relatively maintainable

R. Barnsley et al.

Change of Design to Reduce Neutron Exposure

X-ray Camera - splitting fan view into several sub-views results in improvement in neutron flux at port flange

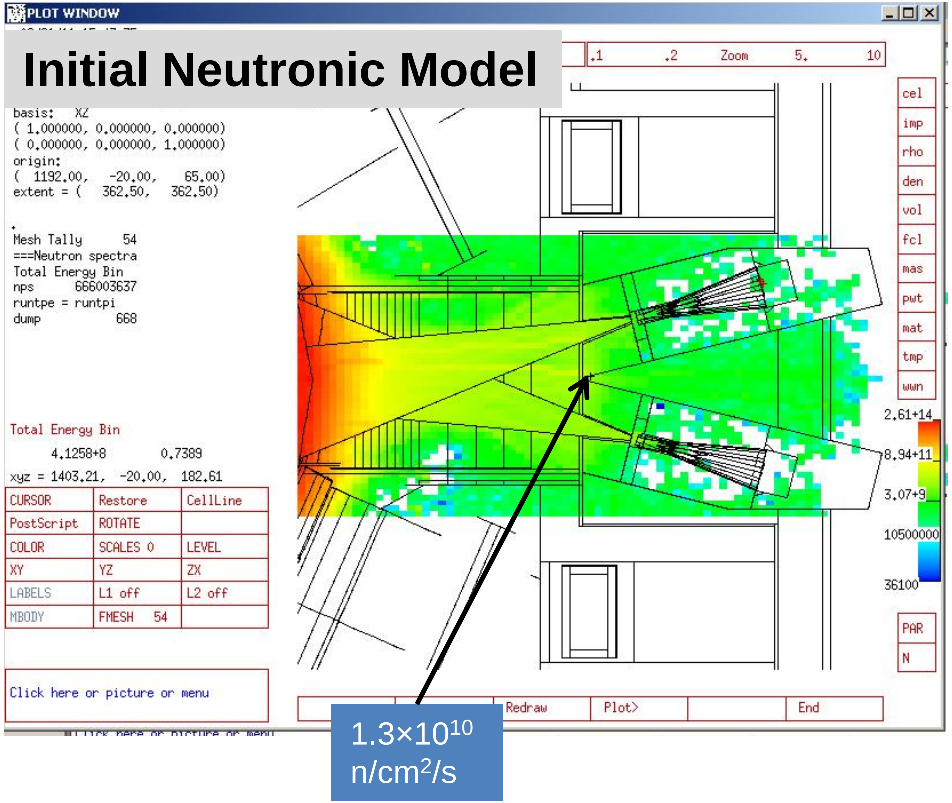

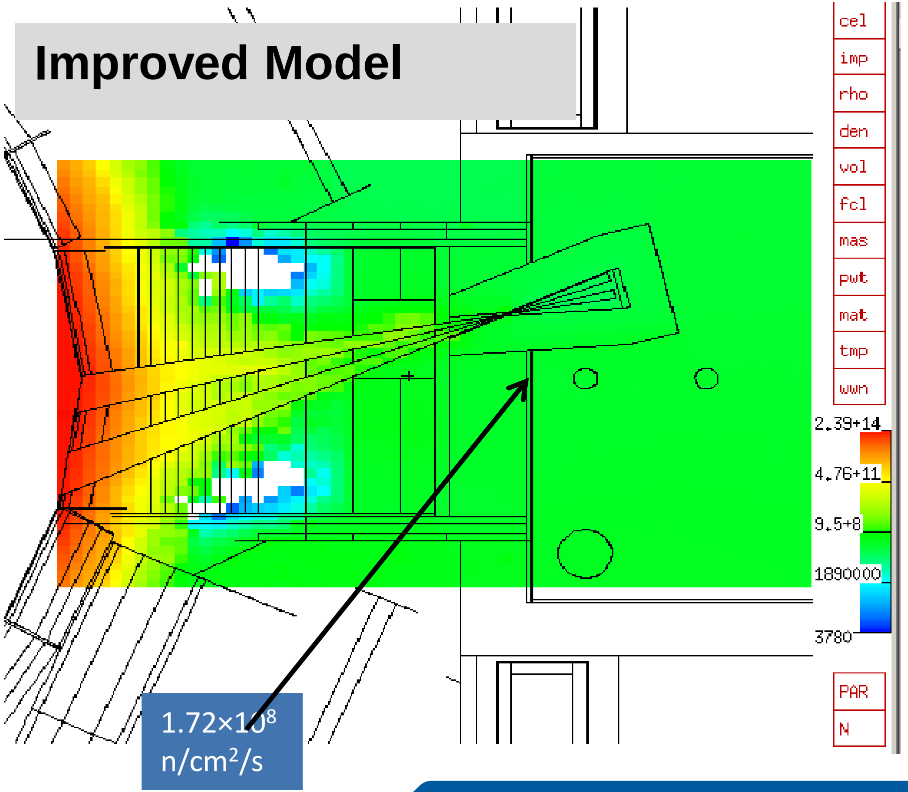

Specific Issue in ITER: Diagnostic Port Coordination

- Different diagnostics share one port – arrangement and coordination (iterative)

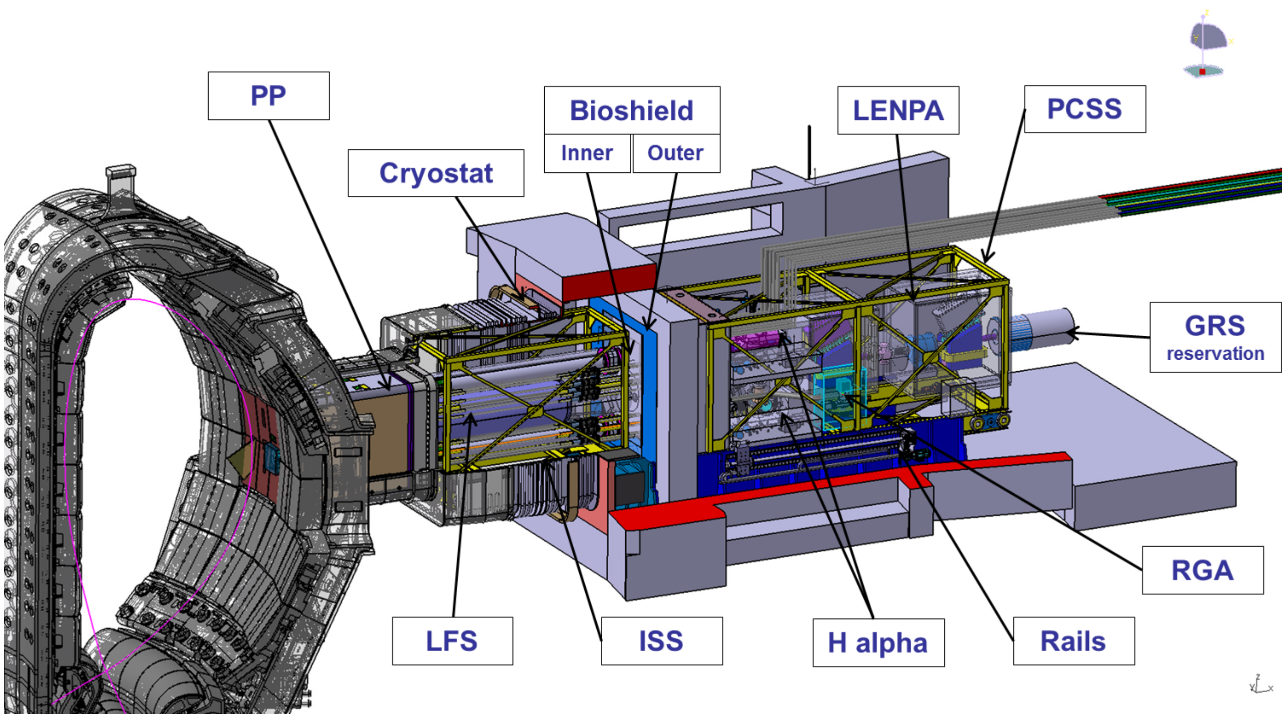

R. Barnsley et al.

Expected Range of Plasma Conditions

- Wide range of plasma backgrounds modelled to reflect operational range of ITER
- Impurity emission is modelled using plasma scenarios as expected targets for diagnostics

- Impurity emission modelling is essential input to designs – sets requirements for instrument:
  - Sensitivity
  - Spectral range and resolution
  - Field of view and spatial resolution

- Continuously refined and expanded
  - Wide range of plasma scenarios
  - Wide range of impurities
  - Impurity radiated power – line and continuum
  - Input to all spectroscopy designs
  - Input to Bolometry design
  - Next step: time resolved simulation of plasma scenarios for synthetic diagnostics, developing and training analysis

ASTRA plasma modelling
ADAS atomic data
SANCO impurity transport

SOLPS solutions in divertor
ERO2.0 PSI at main chamber and divertor

Te (keV)

M. O'Mullane et al.

Emission Modelling in VIS, VUV, SXR and in bolometry

- Sensitivity analysis concerning input parameters (transport) / Variety of plasma conditions
- Complete plasma discharge simulation including intrinsic and extrinsic impurities
- Energy-resolved radiated power predictions to high energies, up to HXR region
- Core, edge, divertor and SOL contributions to total radiation

line of sight SXR emission

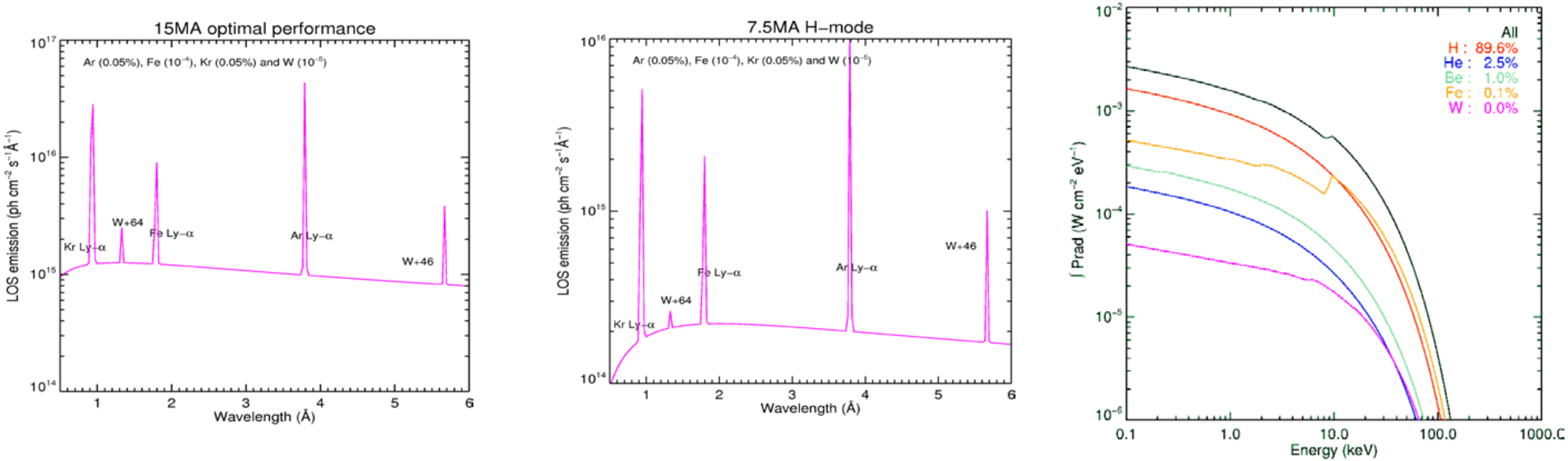

M. O'Mullane et al.

Emission Modelling in VIS, VUV, SXR and in bolometry

- Sensitivity analysis concerning input parameters (transport) / Variety of plasma conditions
- Complete plasma discharge simulation including intrinsic and extrinsic impurities
- Energy-resolved radiated power predictions to high energies, up to HXR region
- Core, edge, divertor and SOL contributions to total radiation

sensitivity of X-ray lines to transport assumptions

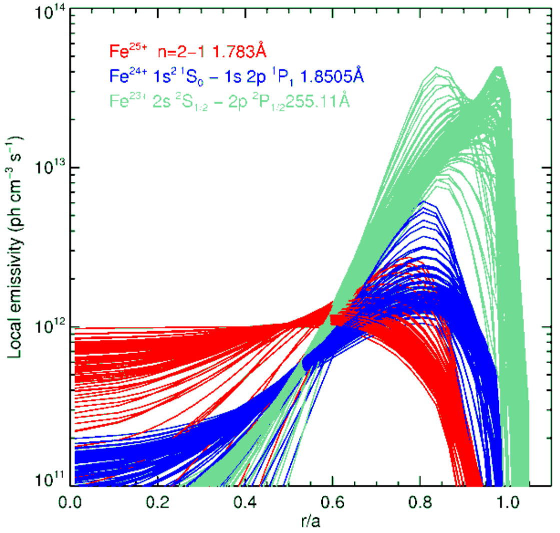

intrinsic vs seed impurities emission in different scenarios

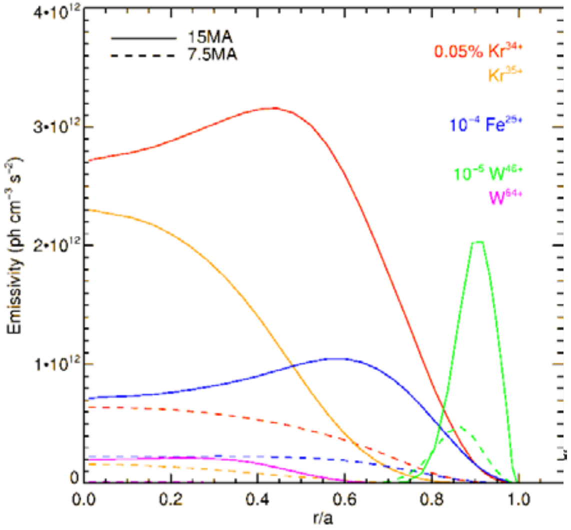

total radiated power

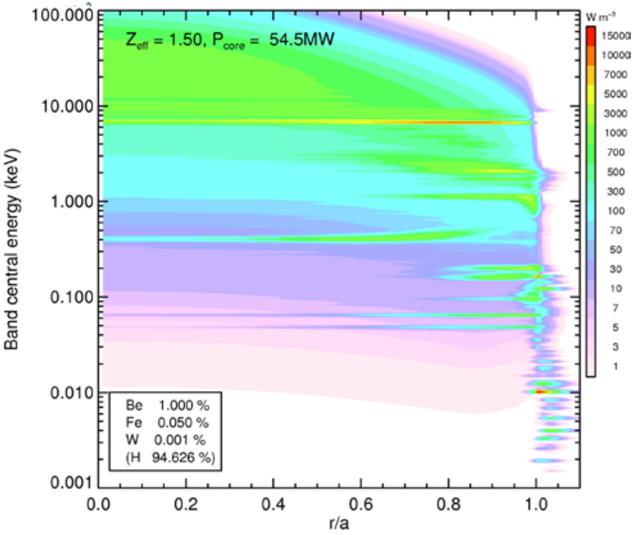

M. O'Mullane et al.

Example: VUV spectroscopy in ITER

- VUV spectrometer system to identify and quantify impurities
- Impurity profiles at pedestal region

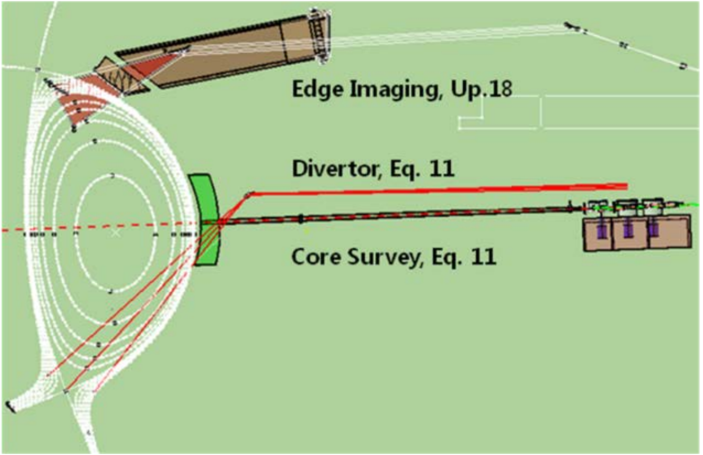

Subsystem	VUV Core survey	VUV Edge imaging	VUV Divertor
PBS	55.E3	55.EH	55.EG
Function	Impurity species identification	Impurity profile	Divertor impurity influxes (W etc.)
Wavelength range (nm)	2.4 – 160	17 – 32	15 - 32
Resolving power ($\lambda/\Delta\lambda$)	~500	~500	~500
Gratings	5	1	1
Implement.	Slot in Eq 11 PP 10 x 100 mm^2 Collimating mirrors in PC	Slot in Up18 PP Field mirror in PP Collimating mirror in PC	Slot in Eq 11 PP Field mirror in PP Collimating mirror in PC

R. Barnsley et al.

Example: VUV spectroscopy in ITER

- Core survey system of HEXOS type with 5 channels
- 5-channel Main Plasma Spectrometers with shielding concept for MCNP analysis

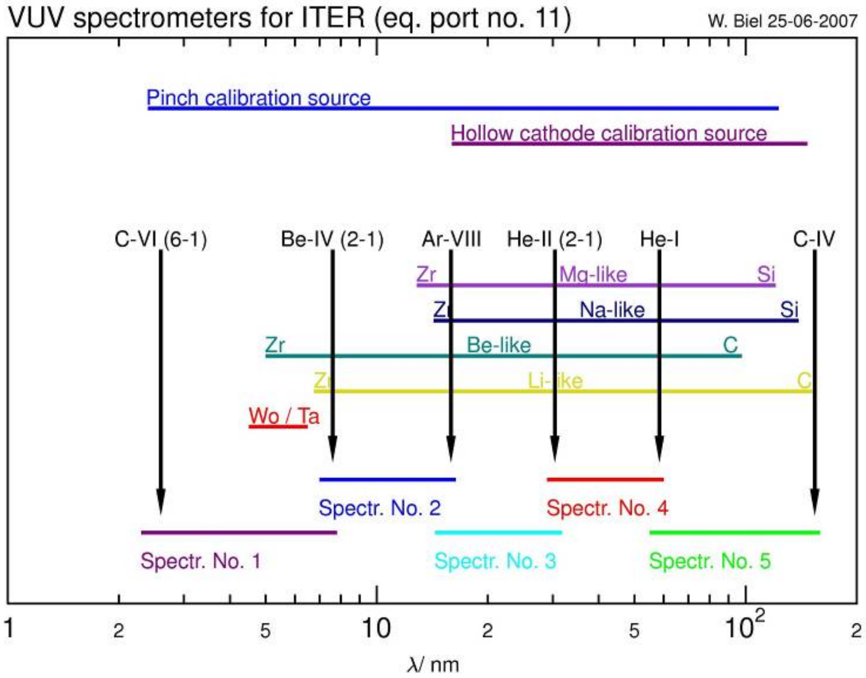

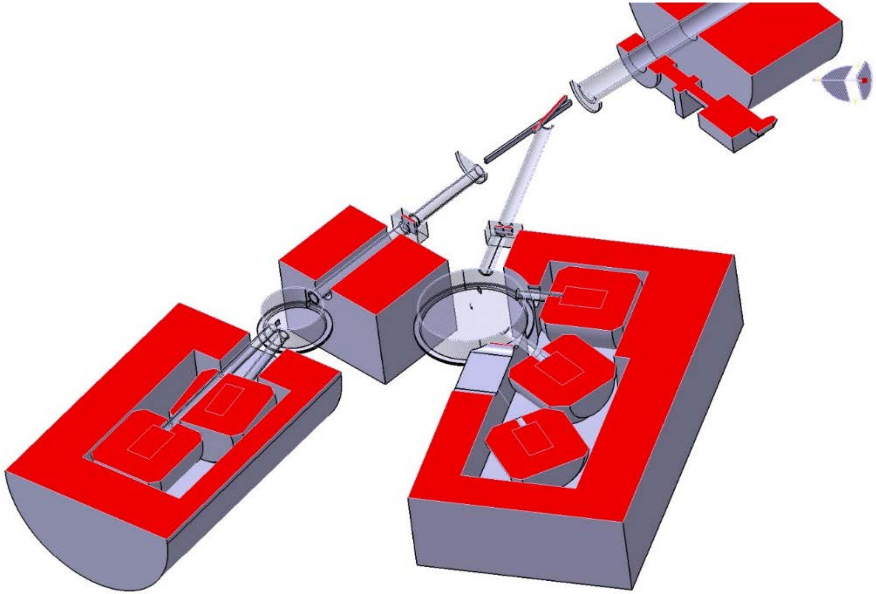

Test of Spectrometer in KSTAR

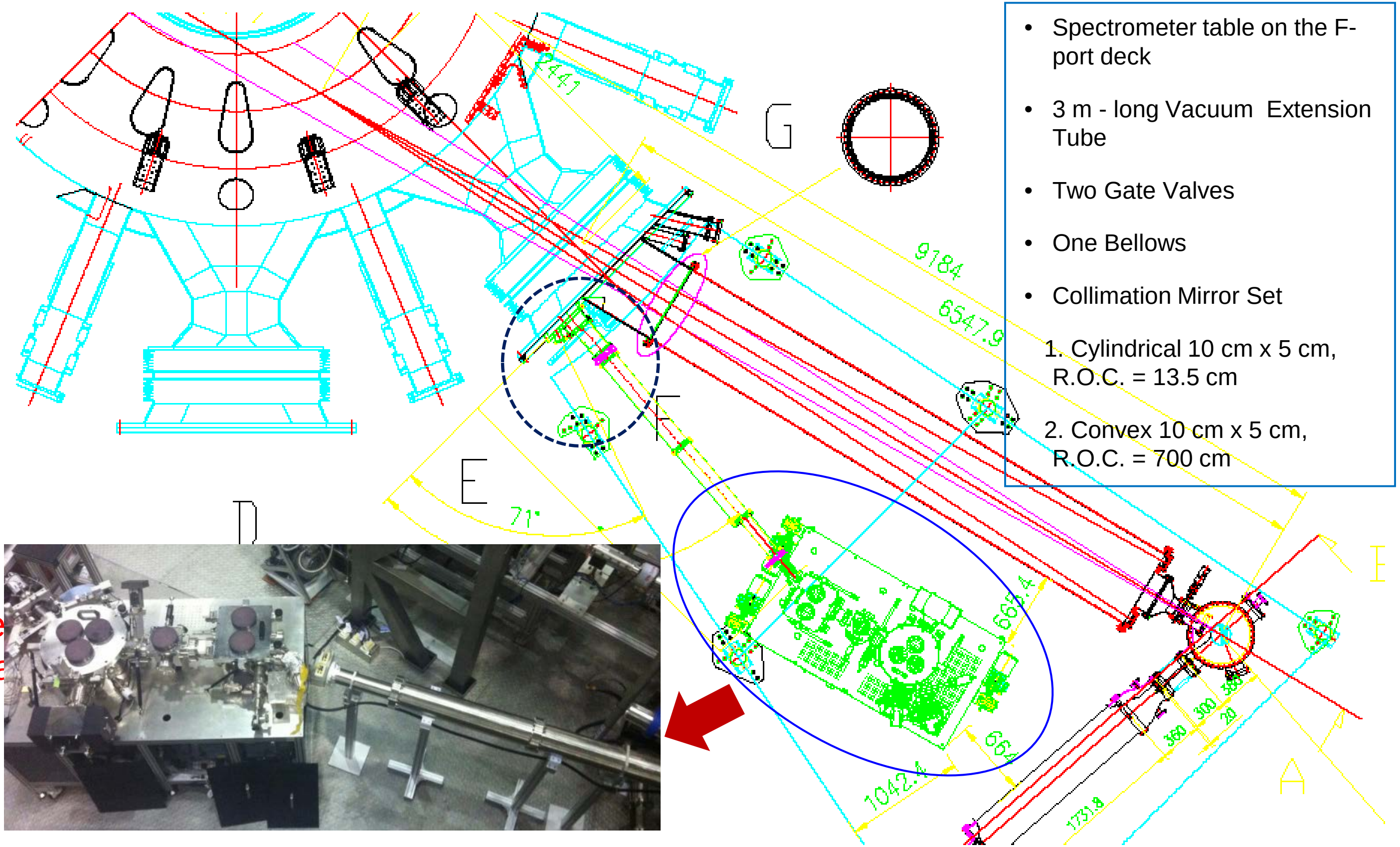

- Spectrometer table on the F-port deck
- 3 m - long Vacuum Extension Tube
- Two Gate Valves
- One Bellows
- Collimation Mirror Set

1. Cylindrical 10 cm x 5 cm, R.O.C. = 13.5 cm
2. Convex 10 cm x 5 cm, R.O.C. = 700 cm

VUV spectromete
on the optica
table

Example Spectra

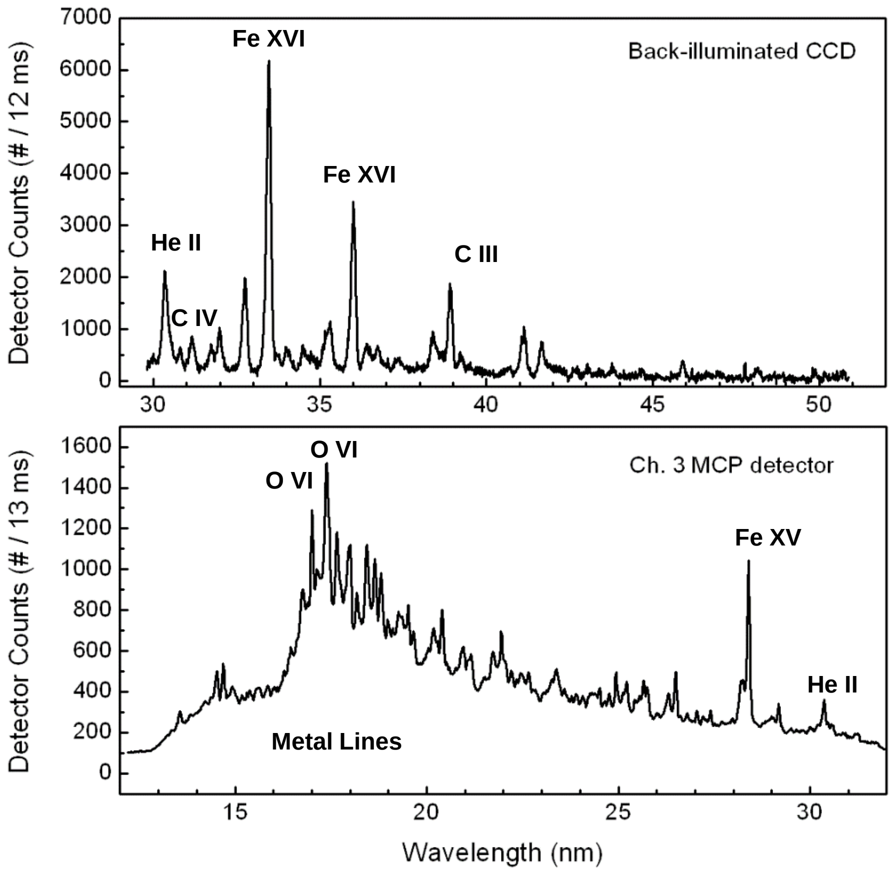

- Impurity lines of initial plasmas at KSTAR 2012 Campaign (2012. 09. 06)

Main Chamber H_{alpha} System

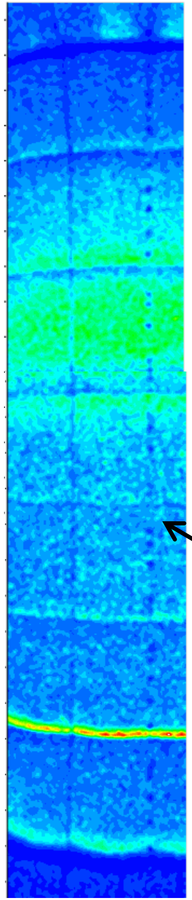

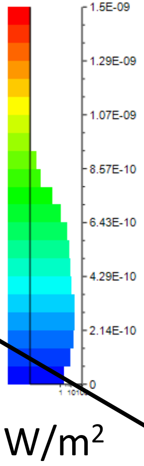

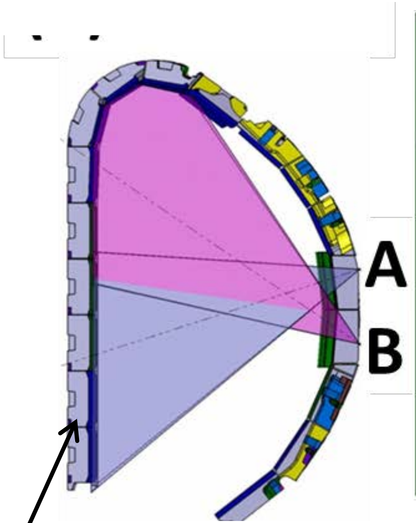

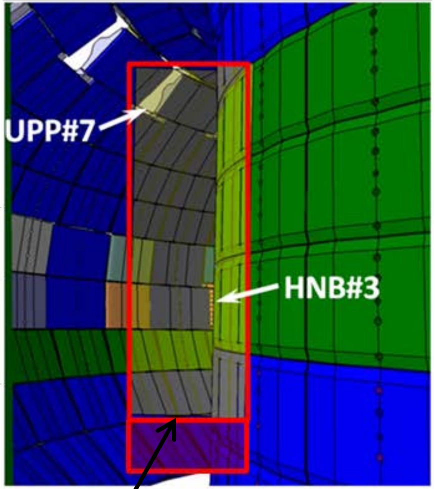

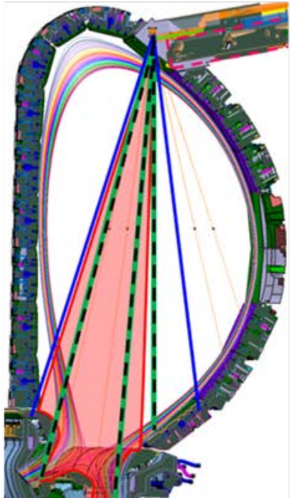

Image features on inner wall

Tangential view most features highest contrast

Divertor view to quantify divertor emission

Reflections for Main H_{alpha} Diagnostic

No reflections

Divertor signal

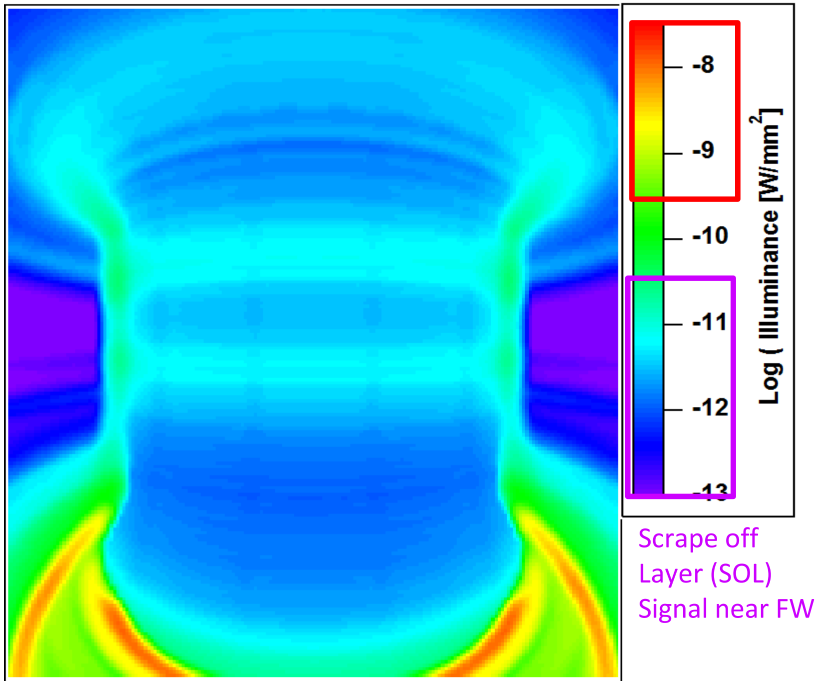

Scrape off Layer (SOL) Signal near FW

With Reflections

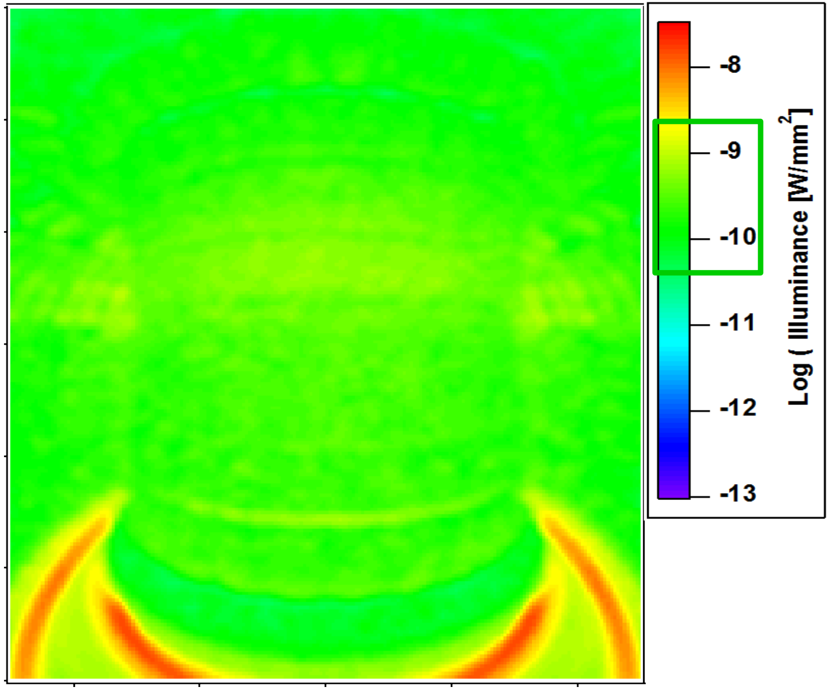

Signal near FW
=
SOL signal
+
reflected signal from divertor

Light tools software

CXRS Systems in ITER

	r/a < 0.6 – 0.7	r/a > 0.5	r/a > 0.85
Name	CXRS-core	CXRS-edge	CXRS-pedestal
Spatial resolution	a/30	a/30 – a/100	a/100

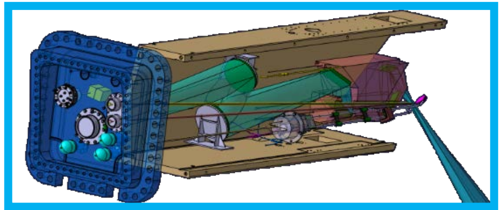

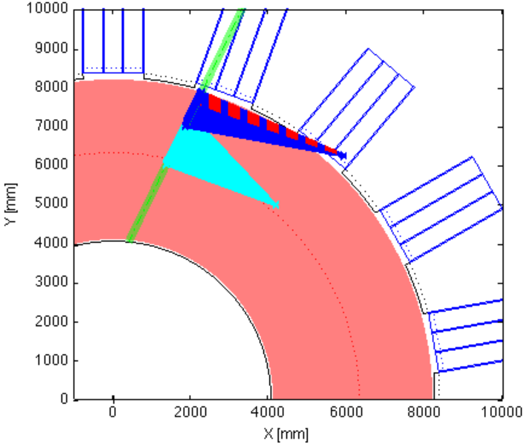

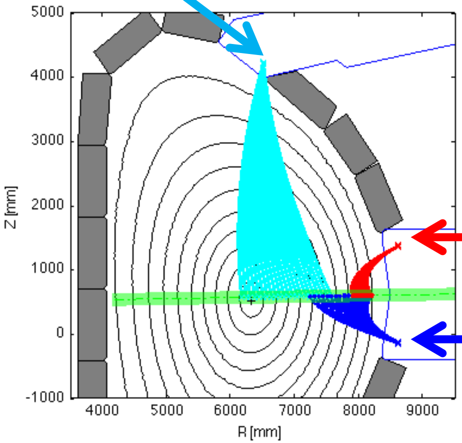

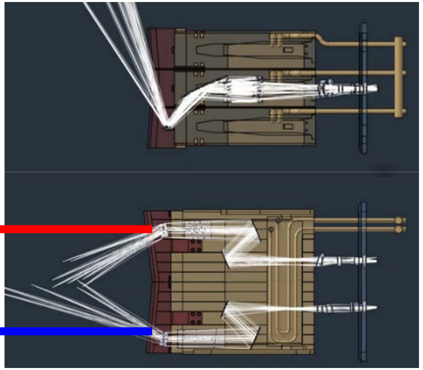

CXRS Core System

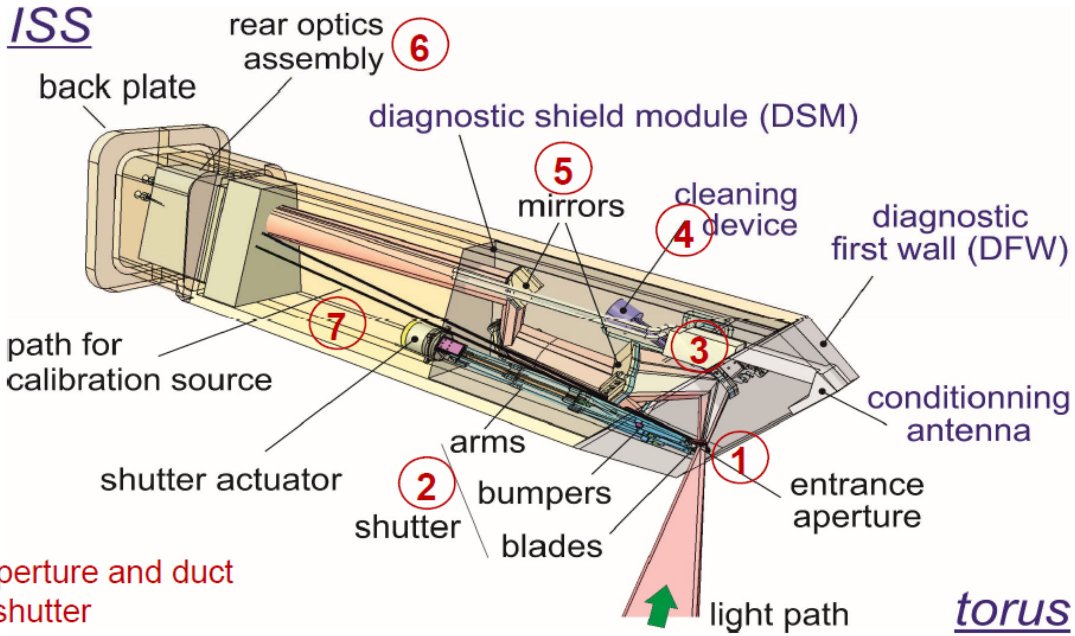

1 entrance aperture and duct
2 protective shutter
3 first mirror M1
4 cleaning device (not in the FPA)
5 mirror chain (M2…Mn)
6 rear optics assembly
7 calibration system

Ph. Mertens et al.

CXRS Core System

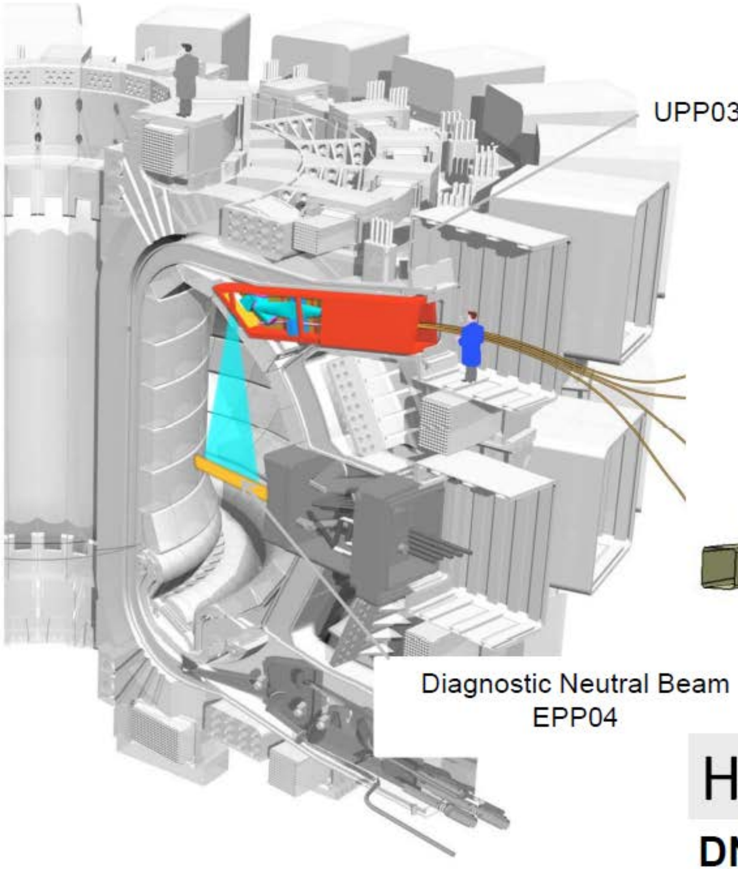

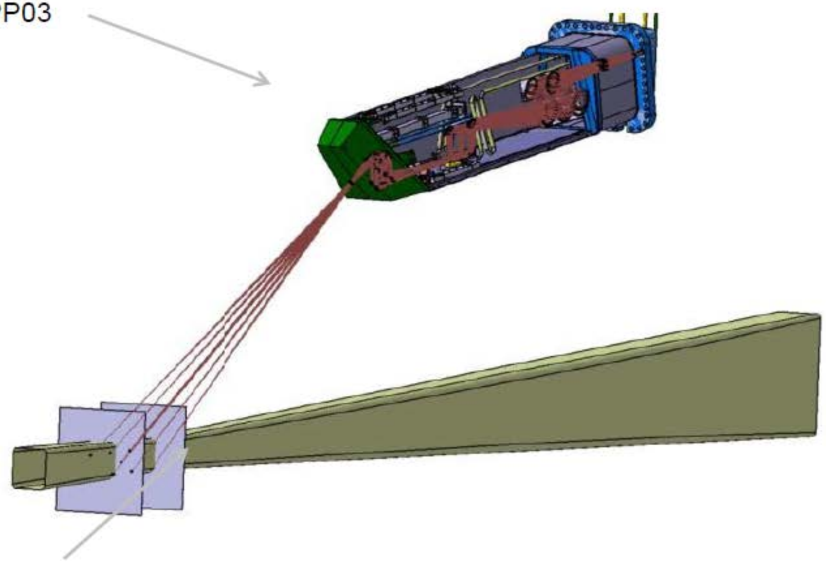

$$H^0 + X^{z+1} \rightarrow H^+ + X^z(nl)^* \rightarrow \hbar\omega$$

DNB (ITER): ≤100 keV/amu, ≥36A, 7 mrad

Ph. Mertens et al.

CXRS Spectral Properties and Quantities

Line width:
Ion temperature

$$T_i = \frac{m_i}{k_B}\left(\frac{c\lambda_w}{\lambda_0\sqrt{8\ln 2}}\right)^2$$

Line shift:
Plasma rotation

$$v_{rot} = -c\frac{\Delta\lambda_{rot}}{\lambda_0}$$

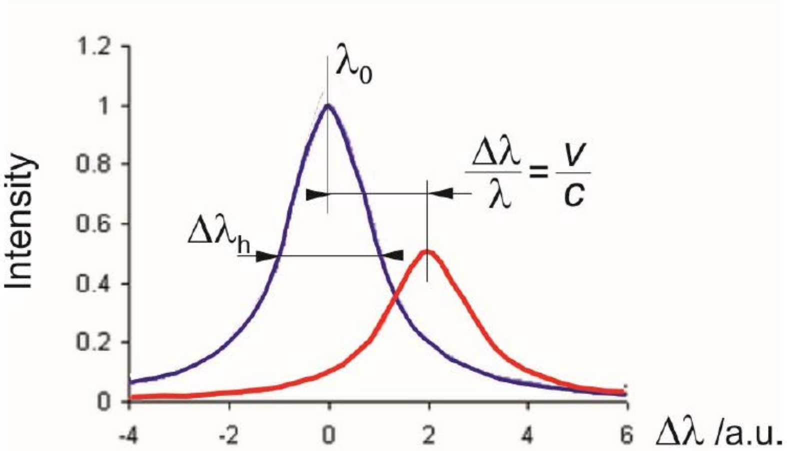

Integral:
Ion density

$$\phi = \frac{1}{4\pi}\int n_{I^{Z+}} n_{beam} \langle \sigma_{em} v_{beam} \rangle d\ell$$

ITER

λ465 nm band (He, Be) – around 468 nm → He II, Be IV

λ520 nm band (C, Ne, Ar, Kr) – around 527 nm → C VI, Be II, Ne X and Ar XVII

λ656 nm band (Balmer) – H_α, D_α, T_α at 656 nm

$\Rightarrow$ High resolution spectrometer
$\Rightarrow$ Each lines-of-sight one spectrometer?

CXRS Signal Expectation

Radiances in $m^{-2}\,s^{-1}\,sr^{-1}\,Å^{-1}$

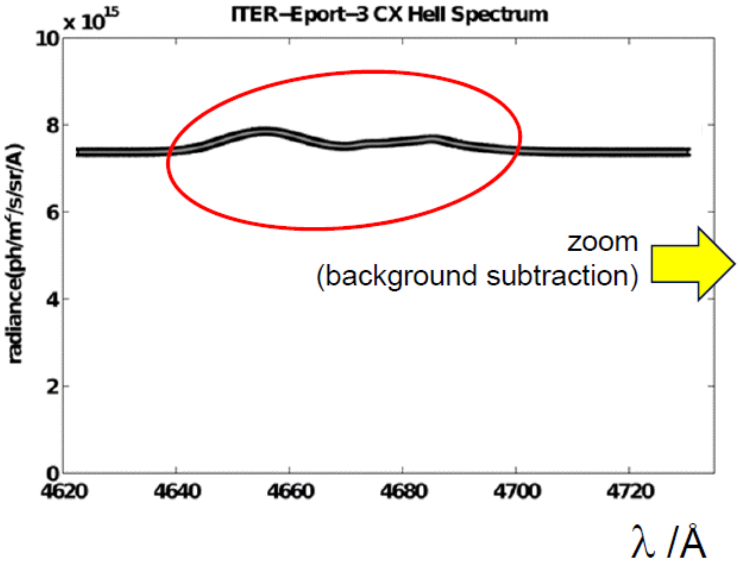

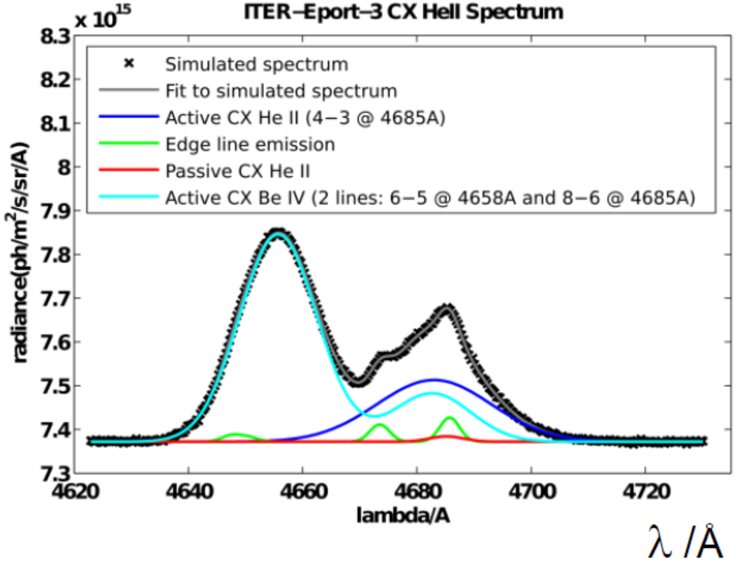

M. De Bock *et al.*, Overview of Active Beam Spectroscopy developments for ITER

Bremsstrahlung: $$B_{\mathrm{LOS}} = \int_{\mathrm{LOS}} dl \int_0^\infty d\lambda\, C\,\overline{g}(\lambda, T_e, Z_{\mathrm{eff}})\, \frac{n_e^2 Z_{\mathrm{eff}}}{\sqrt{k_{\mathrm{B}} T_e}}\, \frac{\exp\left(-\frac{hc}{\lambda k_{\mathrm{B}} T_e}\right)}{\lambda^2}$$

Example: X-Ray Spectroscopy

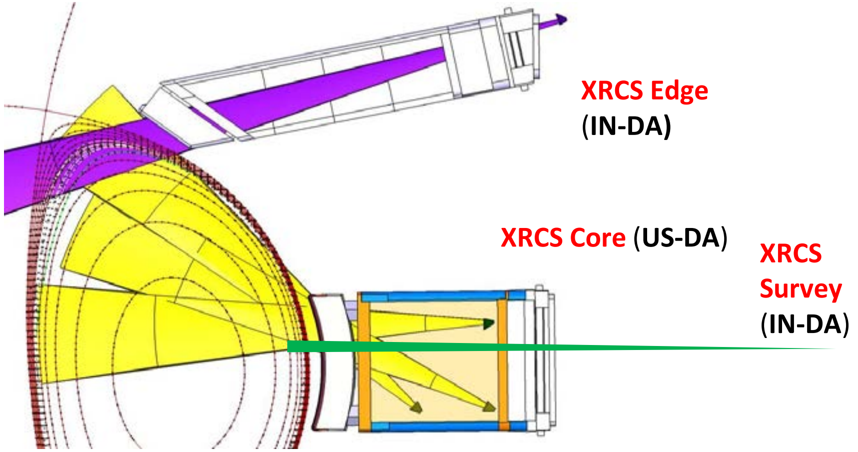

Subsystem	Main plasma x-ray survey	X-ray Core imaging	X-ray Edge imaging
Function	Impurity species identification and monitoring	Core ion temperature, rotation, impurity profile	Edge ion temperature, poloidal rotation, impurity profile
Wavelength range (nm)	0.05 – 10	0.2 – 0.4	0.2 – 0.5
Resolving power (λ/Dλ)	Below 2.5 nm ~1000, Above 2.5 nm ~ 100	~8000	~8000
Implementation	Slot in E11 port-plug, Diffracting optic in port cell	Slot(s) in E09 port-plug, Diffracting optics inside port-plug	Slot in U09 port-plug, Diffracting optic behind the port-plug

Wavelength, 10^{-10}m

Wavelength (A)

ITER x-ray Survey Spectrometer

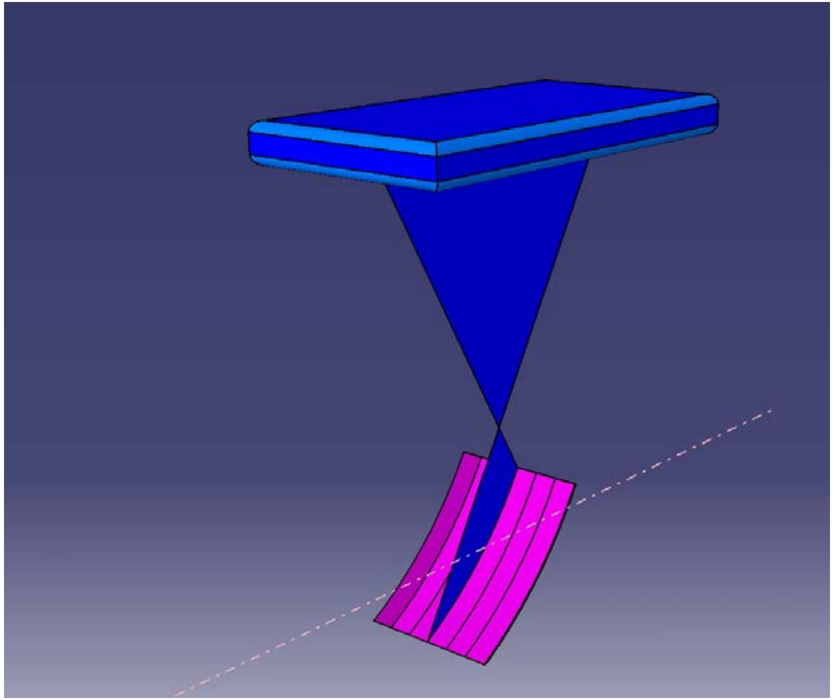

<--- ~ 10 m to slot in blanket

Slot at blanket acts as entrance slit: 10 x 100 mm^2

Range of ~6 different bent crystals with Bragg angle range 30° - 60°

Wavelength coverage ~ 0.05 nm - 10 nm

Spectral resolution ~ 1000 below 2.5 nm, ~ 100 above 2.5 nm

Detectors CCD for long wavelength, Pilatus for short wavelength